의학박사 학위논문

Anti-tumor activity and mechanism of selective CDK4/6 inhibitor in human colorectal cancer cell lines

인간 대장암 세포주에 대한 선택적 CDK4/6 억제제의 항종양효과와 작용기전에 대한 연구

2021 년 2 월

서울대학교 대학원

의학과 의학전공

이 현 정

Anti-tumor activity and mechanism of selective CDK4/6 inhibitor in human colorectal cancer cell lines

인간 대장암 세포주에 대한 선택적 CDK4/6 억제제의 항종양효과와 작용기전에 대한 연구

지도 교수 김 지 현

이 논문을 의학박사 학위논문으로 제출함
2020 년 10 월

서울대학교 대학원
의학과 의학전공
이 현 정

이현정의 의학박사 학위논문을 인준함
2021 년 1 월

위 원 장 이 홍식 (인)
부위원장 김 지 현 (인)
위 원 이 근우 (인)
위 원 고 혜경 (인)
위 원 홍 용사 (인)

Abstract

Anti-tumor activity and mechanism of selective CDK4/6 inhibitor in human colorectal cancer cell lines

Hyun Jung Lee

Molecular Oncology

The Graduate School

Seoul National University

Purpose: Colorectal cancer (CRC) is the third most common cancer and the second highest cause of cancer related mortality worldwide. Selective cyclin dependent kinase (CDK) 4/6 inhibitors have been evaluated as promising therapeutic strategy in many cancers. However, targeting cell cycle regulation in colorectal cancer has not been fully evaluated. The aim of our study was to

investigate the anti-tumor activity of the selective CDK4/6 inhibitors and to explore the mechanism of action of selective CDK4/6 inhibitors in human CRC cell lines.

Materials and Methods: We investigated the anti-proliferative efficacy of selective CDK4/6 inhibitors, palbociclib, abemaciclib, and ribociclib. With the most potent selective CDK4/6 inhibitor, we explored the mechanism of anti-proliferative activity and optimal combination agents with a synergistic interaction in colorectal cancer cell lines. To identify the possible predictive biomarkers for selective CDK4/6 inhibitors, multiple *in vitro* models of colorectal cancer cell lines were used. Tumor xenograft model of human colorectal cancer cell lines were established using athymic nude mice for *in vivo* validation.

Results: Growth inhibition assay with multiple colorectal cancer cell lines revealed that abemaciclib was the most potent among the three selective CDK4/6 inhibitors tested. Abemaciclib monotherapy inhibited cell cycle progression and proliferation especially in Caco-2 and SNU-C4 cells. CDK2-cyclin E complex mediated Rb phosphorylation and AKT phosphorylation appeared to be potential resistance mechanisms to abemaciclib monotherapy. Abemaciclib/BYL719 (selective PI3K p110α inhibitor) combination therapy demonstrated synergistic effects regardless of *PIK3CA* mutation status but showed greater efficacy in the *PIK3CA* mutated SNU-C4 cell line. Growth inhibition, cell cycle arrest, and migration inhibition were confirmed as mechanisms of action for this combination. In a mouse xenograft model with SNU-C4 cell line harboring PIK3CA mutation, abemaciclib/BYL719 combination resulted in tumor growth inhibition and apoptosis with tolerable toxicity.

Conclusion: Abemaciclib showed anti-tumor activity in human colorectal cancer cell lines and dual blockade of PI3K p110α and CDK4/6 showed synergistic anti-tumor effects *in vivo* and *in vitro*. *PIK3CA* mutation could be an additional predictive marker for the efficacy of abemaciclib in combination with BYL719. These findings provide novel insight into a possible therapeutic strategy for patients with metastatic CRC.

Keywords: Colorectal cancer, Abemaciclib, BYL719 (Alpelisib), Cell cycle, Migration, Apoptosis, *PIK3CA*

Student Number: 2013 – 30599

Contents

Results

List of figures

List of tables

List of abbreviations and symbols

ATCC: American Type Culture Collection

CCLE: Cancer Cell Line Encyclopedia

CDK: Cyclin dependent kinase

CI: Combination index

COSMIC: Catalogue Of Somatic Mutations In Cancer

CRC: Colorectal Cancer

DCAFs: D-cyclin-activating features

EGFR: Epithelial growth factor receptor

ER: Estrogen receptor

FBS: Fetal bovine serum

GAPDH: Glyceraldehyde 3-phosphate dehydrogenase

GI_{50}: Single-agent concentration that inhibits cell growth by 50%

GSK-3β: Glycogen synthase kinase-3β

H&E: Hematoxylin and eosin

IC_{50}: Single-agent concentration that inhibits viability by 50%

IHC: Immunohistochemical/ Immunohistochemistry

MAPK: Mitogen-activated protein kinase

MBC: Metastatic breast cancer

MMC: Mitomycin C

mTORC1: Mammalian target of rapamycin complex 1

NSCLC: Non-small cell lung cancer

OS: Overall survival

PBS: Phosphate buffered saline

PI: Propidium iodide

PI3K: Phosphatidylinositol 3-kinases

Rb: Retinoblastoma

rhEGF: Recombinant protein human epithelial growth factor

rhFGF: Recombinant protein human fibroblast growth factor

SDS: Sodium dodecyl sulfate

SEER: US National Cancer Institute Surveillance, Epidemiology, and End Results

TSC: Tuberous sclerosis complex

Introduction

The overall survival (OS) of advanced colorectal cancer (CRC) has improved with the introduction of anti-angiogenic and anti-epithelial growth factor receptor (EGFR) agents since the early 2000's. However, total CRC survival in Korea has plateaued (around 75%) over the past decade [1]. CRC is the third most common in terms of incidence after lung and breast cancer and the second highest in terms of cancer related mortality after lung cancer worldwide [2]. According to the US National Cancer Institute Surveillance, Epidemiology, and End Results (SEER) reports, the 5-year survival of CRC patients with distant metastases is still poor (<15%), whereas the 5-year survival of locoregional disease is approximately 70–90% [3]. This reveals the unmet need of developing effective therapeutic approaches in patients with metastatic CRC after the failure of two kinds of target agents such as anti-angiogenic and anti-EGFR agents.

Cell cycle progression from G_1 to S phase is regulated by cyclin dependent kinase (CDK) 4/6 and cyclin D1 complex-mediated phosphorylation of the retinoblastoma (Rb) tumor suppressor. The intrinsic CDK4/6 inhibitor, p16INK4a, inhibits the enzymatic activity of the CDK4/6-cyclin D1 complex. In cancer cells, the cell cycle is dysregulated by cyclin D1 overexpression, p16 loss, CDK4 mutation, and Rb loss [4]. Similarly, cell cycle dysregulation in CRC is associated with cyclin D1 dysregulation, and a variable frequency of cyclin D1 dysregulation in CRC has been reported according to the types of structural and genetic variants: *CCND1* amplification (2.5%) [5], cyclin D1 overexpression (55%) [6], and genomic

aberrations called D-cyclin-activating features (DCAFs, <10 %) [7]. The expression of cyclin D1 is regulated by several extracellular signaling pathways [8]. In particular, cyclin D levels and CDK4/6 activity are regulated by mitogenic signaling pathways. The mitogen-activated protein kinase (MAPK) pathway promotes cyclin D1 upregulation [9]. MAPK pathway genes *KRAS*, *NRAS*, and *BRAF* represent important molecular targets in colorectal cancer and serve as predictive factor in the identification of patients who potentially benefit from anti-EGFR treatment [10]. In general, mitogenic signaling via the phosphatidylinositol-3-kinase (PI3K)-AKT pathway promote cell proliferation and tumor growth. PI3K—encoded by the *PI3KCA* gene—is activated by different receptor tyrosine kinases (such as IGFR, EGFR, VEGFR, FGFR, and RET) and activates AKT, which leads to inhibition of TSC1/2 (Tuberous sclerosis complex 1/2) and consequently to activation of mTORC1/p70S6K [11]. Mitogenic signaling via the PI3K-AKT pathway also increases cyclin D1 levels by blocking glycogen synthase kinase-3β (GSK-3β)-mediated cyclin D1 proteolysis and subcellular localization [12]. In contrast, the CDK4/6-cyclin D1 complex stimulates mammalian target of rapamycin complex 1 (mTORC1), which is located downstream of PI3K [13]. These findings give rationale for the combination of CDK4/6 inhibitors and mitogenic signaling inhibitors in CRC treatment. Currently, CDK is known as a modifiable key factor of cell cycle transition, and some CDK4/6 inhibitors are used in numerous clinical settings.

This study was designed to investigate the anti-tumor activity of the selective CDK4/6 inhibitors and identify an optimal combination agent with selective CDK4/6 inhibitors in CRC cell lines. In addition, this study was

performed to explore mechanisms of resistance to selective CDK4/6 inhibitors and mechanisms of action for possible combination therapy in CRC cell lines.

Materials and Methods

Materials

Palbociclib, abemaciclib, ribociclib, BYL719, buparlisib, AZD8186, ipatasertib, AZD5363, and MK2206 were purchased from Selleckchem (Houston, TX, USA). Antibodies against the following proteins were purchased from Santa Cruz Biotechnology (Dallas, TX, USA): p107 (sc-250), p130 (sc-9963), cyclin A (sc-751), cyclin D1 (sc-753), cyclin E (sc-481), CDK2 (sc-163), and GAPDH (Glyceraldehyde 3-phosphate dehydrogenase, sc-47724). Antibodies against Rb (cs#9309), p-Rb (cs#8180), E2F (cs#3742), p16 (cs#92803), p-AKT S473 (cs#4058), p-AKT T308 (cs#9275), AKT (cs#4685), p-TSC2 (cs#3617), TSC2 (cs#4308), and vinculin (cs#13901) were purchased from Cell Signaling Technology (Danvers, Massachusetts, USA). Recombinant protein human epithelial growth factor (rhEGF) and recombinant protein human fibroblast growth factor (rhFGF) were purchased from R&D Systems (Minneapolis, MN, USA). Mitomycin C (MMC), propidium iodide (PI), RNase, Leibovitz's L-15, Eagle’s Minimum Essential Medium (EMEM), and sodium dodecyl sulfate (SDS) were purchased from Sigma Aldrich (USA). Phosphate buffered saline (PBS) and fetal bovine serum (FBS) were purchased from Gibco (Grand Island, NY, USA). Roswell Park Memorial Institute (RPMI) 1640 and Dulbecco’s modified Eagle’s medium (DMEM) were purchased from Welgene (Daejeon, South Korea). All chemicals and reagents were of analytical grade and were obtained from commercial sources.

Cell culture

HCT-15, DLD-1, HCT-8, SW480, SNU-175, SNU-C5, HT-29, Caco-2, SNU-C2B, Lovo, Colo320DM, and SNU-C4 cells were purchased from the Korean Cell Line Bank (Seoul, South Korea). SW48 cells were purchased from American Type Culture Collection (ATCC, Manassas, VA, USA). DiFi cell line was kindly provided by Prof. Joonoh Park at Sungkyunkwan University, Seoul, Republic of Korea.

HCT-15, DLD-1, HCT-8, SW480, SNU-175, SNU-C5, HT-29, Lovo, SNU-C2B, Colo320DM, and SNU-C4 cells were maintained in RPMI 1640 with 10% FBS, 4mM L-glutamine, and 1% penicillin/streptomycin at 37°C with 5% CO2. SW48 was maintained in Leibovitz's L-15 with 10% FBS, and 1% penicillin/streptomycin at 37°C with 100% air. Caco-2 cells were maintained in DMEM with 10% FBS, 4mM L-glutamine, and 1% penicillin/streptomycin at 37°C with 5% CO2. Normal colon epithelial CCD8410CoN cell line was kindly provided by Prof. Nayoung Kim at Seoul National University, Seoul, Republic of Korea. CCD841CoN cells were maintained in an EMEM with 10% FBS, 4mM L-glutamine, and 1% penicillin/streptomycin at 37°C with 5% CO2.

Cell proliferation assay

The cell proliferation assay was performed using the CellTiter-Glo Luminescent Cell Viability Assay (Promega, Madison, WI, USA) according to manufacturer’s instructions. On day 0, 96-well plates were seeded with 3,000 cells/well and incubated overnight. The next day, cells were treated

with the indicated compounds. On day 4, plates were incubated for 1 h at room temperature, and 100 μL of CellTiter-Glo reagent was added to each well, followed by mixing on an orbital shaker for 5 min. Luminescence was measured on a GloMax 96-well luminometer from Promega (Madison, WI, USA).

Colony-forming assay

Caco-2 and SNU-C4 cells were seeded into 6-well plates and grown for 72 h before being subjected to the indicated treatments for 10 days, and the media was changed at regular time intervals. After 10 days of culture at 37°C with 5% CO2, colonies were washed with PBS, stained with Coomassie Brilliant Blue for 30 min at room temperature, then washed with water, and air-dried. The colonies were photographed using the ChemiDoc Touch (Bio-Rad) and measured using ImageJ software (National Institutes of Health, Bethesda, MD, USA).

Cell migration assay

Caco-2 and SNU-C4 cells were seeded into 96-well plates and grown for 24 h. Confluent monolayers were gently scratched using a WoundMaker (Essen Bioscience, Ann Arbor, MI, USA). Cells were washed twice with PBS to remove floating cells and then incubated for 40 h in growth medium supplemented with 10 ng/mL rhEGF, 10 ng/mL rhFGF2, and 10 μg/mL MMC. The rate of cell migration was expressed as the area of the scratch

relative to total area of the cell-free region immediately after the scratch using IncuCyte Zoom (Essen Bioscience).

Cell cycle analysis

Caco-2 and SNU-C4 cells were seeded into 100-mm plates and grown overnight and were then subjected to the indicated drug treatments for 48 h. After trypsinization, cells were washed twice in PBS, fixed overnight at 4°C in ethanol, washed three times with PBS, and incubated in PBS containing 20 μg/mL PI and 100 μg/mL RNAse at 37°C for 30 min. After washing in PBS, cells were resuspended in 1 mL PBS and examined using a FACSCalibur flow cytometer (BD Biosciences, Franklin Lakes, NJ, USA). Cell cycle distribution was determined using FlowJo software (Tree Star, Ashland, OR, USA).

Combination index analysis

HT-29, Caco-2, and SNU-C4 cells were seeded into 96-well plates at 3,000 cells/well in a total volume of 100 μL basal media containing 10% FBS. The following day, cells were treated in pentaplicate with single agents and their fixed-ratio combination for 72 h over a seven-point titration, which was centered on the single-agent concentrations that inhibited viability by 50% (IC_{50}). Cell viability was measured by the CellTiter-Glo Luminescent Cell Viability Assay (Promega, Madison, WI, USA) according to manufacturer's instructions. Combination index (CI) scores were calculated as previously

described [14] using CalcuSyn software (Biosoft). This software uses the Chou-Talalay combination index method, which is based on the median-effect equation, itself a derivation from the mass-action law. For this analysis, abemaciclib was combined with BYL719 at a constant ratio determined by GI_{50} abemaciclib/IC_{50} BYL719. We entered the resulting proliferation data, along with the data obtained from single drug treatments, into CalcuSyn to determine a CI value for each combination point, which quantitatively defines synergy (CI < 1), additivity (CI = 1), and antagonism (CI > 1).

Western blot analysis

Colon cancer cell lines lysates were obtained by centrifugation at 12,000 × g for 30 min at 4°C. Protein concentration in the supernatant was measured by Bradford assay (BioLegend, San Diego, CA, USA). Proteins (20 μg) were separated by SDS polyacrylamide gel electrophoresis, transferred to a polyvinylidene difluoride membrane (Bio-Rad, Hercules, CA, USA) that was blocked in blocking buffer containing 5% skim milk, and then probed overnight with primary antibodies. Secondary antibodies conjugated with horseradish peroxidase (1:4,000 dilution; Bio-Rad) were applied for 1 h. Immunoreactivity was detected by enhanced chemiluminescence (Biosesang, Seongnam, South Korea) and a ChemiDoc Touch imager (Bio-Rad).

Mouse xenograft

All mice were housed in a specific pathogen-free facility at the Seoul National University Bundang Hospital, Seongnam, Republic of Korea. The project was approved by the Institutional Animal Care and Use committee of Seoul National University Bundang Hospital (IACUC approval number: 51-2018-046). For xenograft mouse studies, male athymic nude mice, weighing 26–28 g (5 weeks old), were purchased from Orient Bio Co. (Kapyong, Republic of Korea). Mice were provided with NIH-07 rodent chow (Zeigler Brothers, Gardners, PA, USA) purchased from Central Lab Animal Inc. (Seoul, Republic of Korea). Animals were acclimated to temperature (20–24°C) and humidity (44.5–51.8%) and a 12-h light/dark cycle for 1 week prior to use. SNU-C4 cells (1×10^7) were subcutaneously implanted with Matrigel (BD Biosciences, San Jose, CA) into the flank of each mouse. Ten days after cell inoculation, when palpable tumors were observed, mice were randomly assigned to receive one of the following treatments: (A) three times weekly oral administration of vehicle, i.e., sterile water (control group), (B) daily oral administration of abemaciclib (25 mg/kg/day of body weight) in sterile water, (C) daily oral administration of abemaciclib (50 mg/kg/day of body weight) in sterile water, (D) daily oral administration of BYL719 (15 mg/kg/day of body weight) in sterile water, (E) daily oral administration of BYL719 (30 mg/kg/day of body weight) in sterile water, (F) daily oral administration of abemaciclib (25 mg/kg/day of body weight) combined with BYL719 (15 mg/kg/day of body weight) in sterile water, or (G) daily oral administration of abemaciclib (50 mg/kg/day of body weight) combined with BYL719 (30 mg/kg/day of body weight) in sterile water. The mice (five per treatment group) were weighed, and tumor

areas were measured throughout the study. Treatments were continued for 4 weeks, and the mice were euthanized by CO2 asphyxiation, weighed, and subjected to necropsy. The volume and weights of xenograft tumors were recorded. Selected tissues were further examined by routine hematoxylin and eosin (H&E) staining and immunohistochemical (IHC) analyses.

Immunohistochemistry

Paraffin-embedded tissue blocks from the xenograft tumors were extracted and sectioned at a thickness of 5 μm. Tissue sections from mouse xenograft tumors, mounted on poly-L-lysine-coated slides, were deparaffinized by standard methods. Endogenous peroxidase was blocked by 3% hydrogen peroxide in PBS for 10 minutes. Antigen retrieval was done for 5 minutes in 10 mM sodium citrate buffer (pH 6.0) heated at 95°C in a steamer, followed by cooling for 15 minutes. Slides were washed with PBS and incubated for 1 hour at room temperature with a protein-blocking solution (VECTASTAIN ABC kit, Vector Laboratories, Burlingame, CA, USA). Excess blocking solution was drained, and samples were incubated overnight at 4°C with one of the following: a 1:500 dilution of p-AKT S473 and KI67 antibodies. Sections were then incubated with biotinylated secondary antibody followed by streptavidin (VECTASTAIN ABC kit). Color was developed by exposing the peroxidase to diaminobenzidine reagent (Vector Laboratories), which forms a brown reaction product. Sections were then counterstained with Gill's hematoxylin (Sigma) for 1 minute. Brown staining identified p-AKT S473, and KI67 expression.

Apoptosis assay

TUNEL (terminal deoxynucleotidyl transferase dUTP nick end labeling) assay was used to detect apoptotic cells and performed with ApopTag® Peroxidase *In situ* Apoptosis detection kit. Paraffin-embedded tissue blocks from the xenograft tumors were extracted and sectioned at a thickness of 5 μm. Tissue sections from mouse xenograft tumors, mounted on poly-L-lysine-coated slides, were deparaffinized and washed according to manufacturer's manual. Endogenous peroxidase was blocked by 3% hydrogen peroxide in PBS for 5 minutes in room temperature. Tissues were treated with equilibration buffer and incubated for 10 seconds at room temperature. Slides were washed with PBS and incubated for 1 hour at 37 ℃ with terminal deoxynucleotidyl transferase (TdT) enzyme in a humidified chamber followed by incubation with anti-digoxigenin conjugate in a humidified chamber for 30 minutes at room temperature. Color was developed by exposing the peroxidase to diaminobenzidine reagent (Vector Laboratories), which forms a brown reaction product. Sections were then counterstained with Gill's hematoxylin (Sigma) for 1 minute.

Statistical analysis

Statistical analyses were performed using SPSS v.12.0 software (SPSS Inc., Chicago, IL, USA). One-way analysis of variance was used for comparisons among groups. Significant differences between mean values were assessed with Duncan's test. A p-value < 0.05 was considered statistically significant.

The Student's *t-test* was also used to compare two independent groups. *$p < 0.05$; **$p < 0.01$; or ***$p < 0.001$.

Results

Abemaciclib is the most potent selective CDK4/6 inhibitor in human colorectal cancer cell lines

The growth inhibitory activity of palbociclib, abemaciclib and ribociclib were evaluated in 14 human CRC cell lines. These CRC cell lines harbored distinct genetic alterations **(Table 1)**. Key genetic alterations which could be possible predictive markers for response to selective CDK4/6 inhibitors were obtained from the Cancer Cell Line Encyclopedia (CCLE) database [15] and Catalogue Of Somatic Mutations In Cancer (COSMIC) database [16].

Abemaciclib **(Figure 1B)** seemed to be the most potent among the three selective CDK4/6 inhibitors, followed by palbociclib **(Figure 1A)**. Mean GI_{50} of abemaciclib, palbociclib, and ribociclib were 2.05 μM (range, 0.07 – 8.45), 4.14 μM (range, 0.09 – 10.67), and 17.7 μM (range, 1.18 – 47.41), respectively. Most of the human colorectal cancer cell lines tested were initially resistant to ribociclib in growth inhibition assay **(Figure 1C)**. *KRAS* wild-type colorectal cancer cell lines (Red letters in Figure 1) showed tendency to be more sensitive to abemaciclib **(Figure 1B)**.

Table 1. Key genetic alterations in each of the colorectal cancer cell lines

	HCT-15	DLD-1	HCT-8	SW480	SNU-175	SNU-C2B	LoVo	SNU-C5	HT-29	Caco-2	SNU-C4	DiFi	Colo320DM	SW48
MSI status	MSI	MSI	MSI	MSS	MSI			MSI	MSS	MSS	MSI		MSS	MSI
KRAS	G13D	G13D	G13D	G12V	A59T	G12D	G13D	WT	WT	WT	WT	WT	WT	WT
BRAF	WT	WT	WT	WT	WT	WT	G70G	V600E	V600E T119 S	WT	D22N	WT	WT	WT
PIK3CA	E545K	E545K	E545K	WT	WT	D725G	WT	H1047R	P449T	WT	E545G	WT	WT	WT
	D549N	D549N	D549N								V71I			
PTEN	WT	WT	WT	WT	WT	WT	WT	WT	WT	WT	E288fs	WT	WT	WT
											F241S			
TP53	S241F	S241F	WT	R273H	WT	R273H	WT	R248W	R273H	p.C135F	G245S	K132R	R248W	WT
				P309S		R273C		V218L		p.E204*				
						S185S								
ERBB2	WT	-	WT	E1229*	R1146W	R678Q	WT	WT	WT	WT	WT	WT	WT	WT
ERBB3	R667H	-	WT	WT	WT	WT	WT	I65M	WT	D857N	WT	WT	WT	WT
	N126K													
	P1142H													
ERBB4	T716T	WT	WT	WT	R1250W	WT	R782Q	WT	WT	WT	N1062S	WT	WT	P1196S
	L369I				G1069G									

Figure 1. GI_{50} concentrations of selective CDK4/6 inhibitors for each of the colorectal cancer cell lines

Each of the colorectal cancer cells were exposed to palbociclib (A), abemaciclib (B), and ribociclib (C) at the indicated concentrations for 5 days. GI_{50} concentrations were calculated using CalcuSyn software.

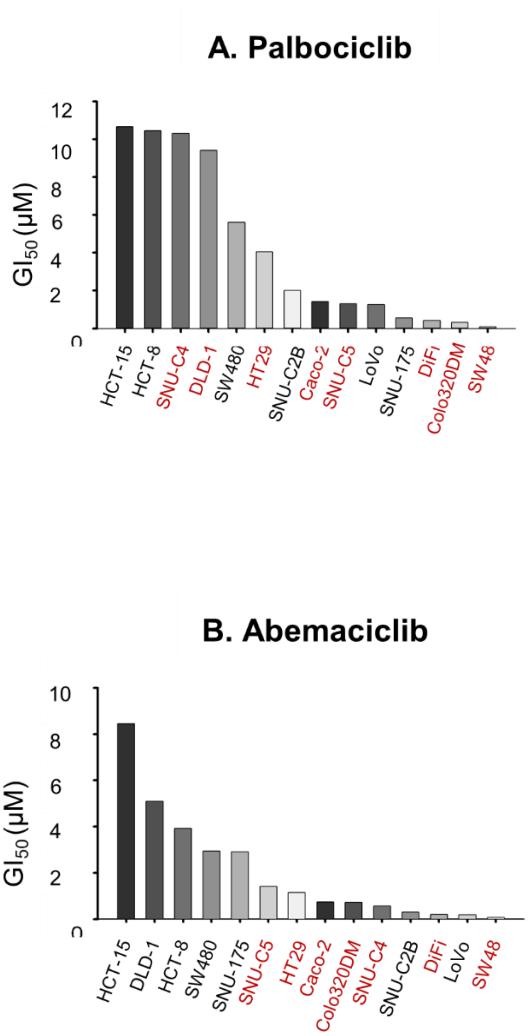

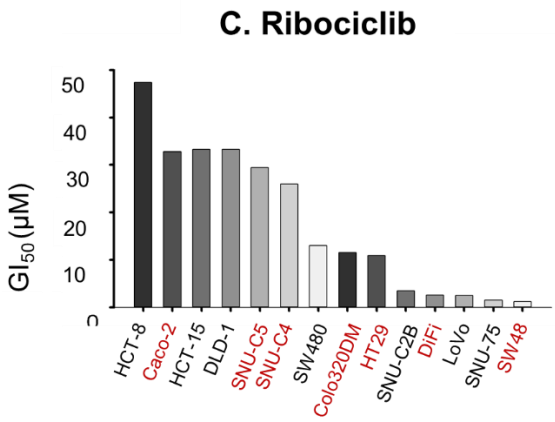
C. Ribociclib
GI50 (μM)
50
40
30
20
10
0
HCT-8
Caco-2
HCT-15
DLD-1
SNU-C5
SNU-C4
SW480
Colo320DM
HT29
SNU-C2B
DiFi
LoVo
SNU-75
SW48

Abemaciclib differentially regulates cell proliferation depending on cyclin D1 and p16 expression in colorectal cancer cell lines

We examined the anti-proliferative activity of abemaciclib in human normal colon epithelial CCD841CoN cell line and CRC cell lines according to sensitivity. As shown in **Figure 2A**, the anti-proliferative effect of abemaciclib was relatively higher in SNU-C4, Caco-2, HT-29, and SNU-C5 cell lines ($GI_{50} \leq 2.0$ μM) compared with the SNU-175, SW480, HCT-8, DLD-1, and HCT-15 cell lines ($GI_{50} > 2.0$ μM). Whereas abemaciclib was approximately three to fifteen fold less toxic against normal colon epithelial CCD841CoN cell compared with CRC cell lines.

Cyclin D1 expression was higher in some abemaciclib-resistant cell lines (HCT-15, DLD-1, HCT-8, and SW480). HCT-15 was the most resistant cell line, and it also showed high p16 expression and low Rb expression **(Figure 2B)**. Abemaciclib-sensitive cell lines (SNU-C5, HT-29, Caco-2, and SNU-C4) reported some common features, including intact Rb expression and relatively low cyclin D1 and p16 expression, when compared with the resistant HCT-15 cell line. As more clinically relevant *in vitro* models, Caco-2 and SNU-C4 cells, which showed the lowest GI_{50} concentrations (<1 μM) in our experiment, were selected.

Figure 2. Effect of abemaciclib on cell viability and cell cycle in colorectal cancer cell lines

(A) Cells were exposed to abemaciclib at the indicated concentrations for 5 days. GI_{50} concentrations were calculated using CalcuSyn software.

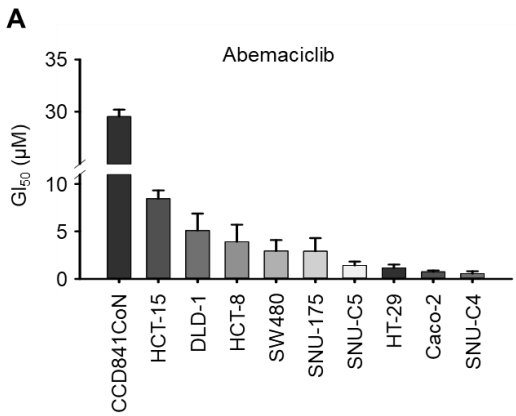

(B) The protein expression levels of Rb, cyclin D1, p16, and GAPDH were evaluated in HCT-15, DLD-1, HCT-8, SW480, SNU-176, SNU-C5, HT-29, Caco-2, and SNU-C4 cells. GAPDH was used as a protein-loading control.

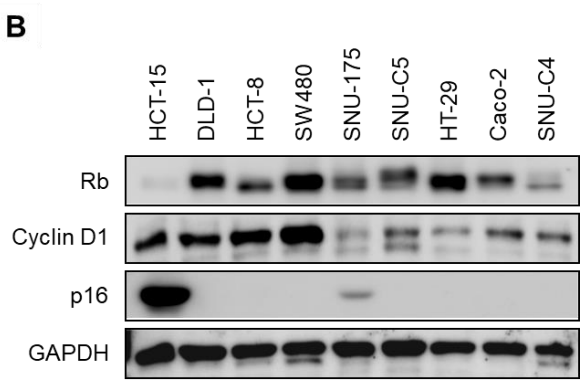

Among the abemaciclib-sensitive CRC cell lines, all four cell lines lacked mutations in *CCND1*, *RB1*, and *KRAS*. The *CDKN2A* gene was wild-type in HT-29, Caco-2, and SNU-C4 cells, but not in SNU-C5 cells, which harbor a *CDKN2A*-silencing mutation. HT-29 and SNU-C4 cells were confirmed to have *BRAF* and *PIK3CA* mutations concurrently **(Table 2)**.

Table 2. Genetic alterations in colorectal cancer cell lines according to sensitivity to abemaciclib

	Primary resistance cell lines to CDK4/6 inhibitors					Sensitive cell lines to CDK4/6 inhibitors			
	HCT-15	**DLD-1**	**HCT-8**	**SW480**	**SNU-175**	**SNU-C5**	**HT-29**	**Caco-2**	**SNU-C4**
CCND1	WT	-	-	WT	WT	WT	WT	WT	WT
CDKN2A	WT	-	-	WT	DEL	Silent	WT	WT	WT
RB1	WT	-	-	WT	R798Q D921D	WT	WT	WT	WT
KRAS	G13D	G13D	G13D	G12V	A59T	WT	WT	WT	WT
BRAF	WT	WT	WT	WT	WT	V600E	V600E T119S	WT	D22N
PIK3CA	E545K D549N	E545K D549N	E545K D549N	WT	WT	H1047R	P449T	WT	E545G V71I
PTEN	WT	WT	WT	WT	WT	WT	WT	WT	F288fs F288S

Cell cycle analysis was performed by flow cytometry to confirm the effect of abemaciclib on cell cycle progression. Abemaciclib treatment for 48 h increased the fraction of Caco-2 and SNU-C4 cells in the G_0/G_1 phase and decreased that of cells in the S phase **(Figure 3)**. A cell cycle regulation-related gene expression assay revealed that Rb phosphorylation in Caco-2 and SNU-C4 cells decreased after exposure to abemaciclib. Cyclin E and CDK2 expression were not affected by abemaciclib treatment in Caco-2 and SNU-C4 cells **(Figure 4)**. Moreover, we conducted colony-forming assays to evaluate the long-term effects of abemaciclib on CRC cell lines. Colony formation in Caco-2 and SNU-C4 cells decreased after abemaciclib treatment in a dose-dependent manner **(Figure 5)**.

Figure 3. Effect of abemaciclib on cell cycle progression

Cell cycle analysis was conducted by FACScalibur after propidium iodide (PI) staining. A total of 2 × 10^6 cells was seeded into 100-mm plates and treated with or without abemaciclib. Data are presented as histograms (black, 0 μM abemaciclib; gray, 1 μM abemaciclib; dark gray, 5 μM abemaciclib.

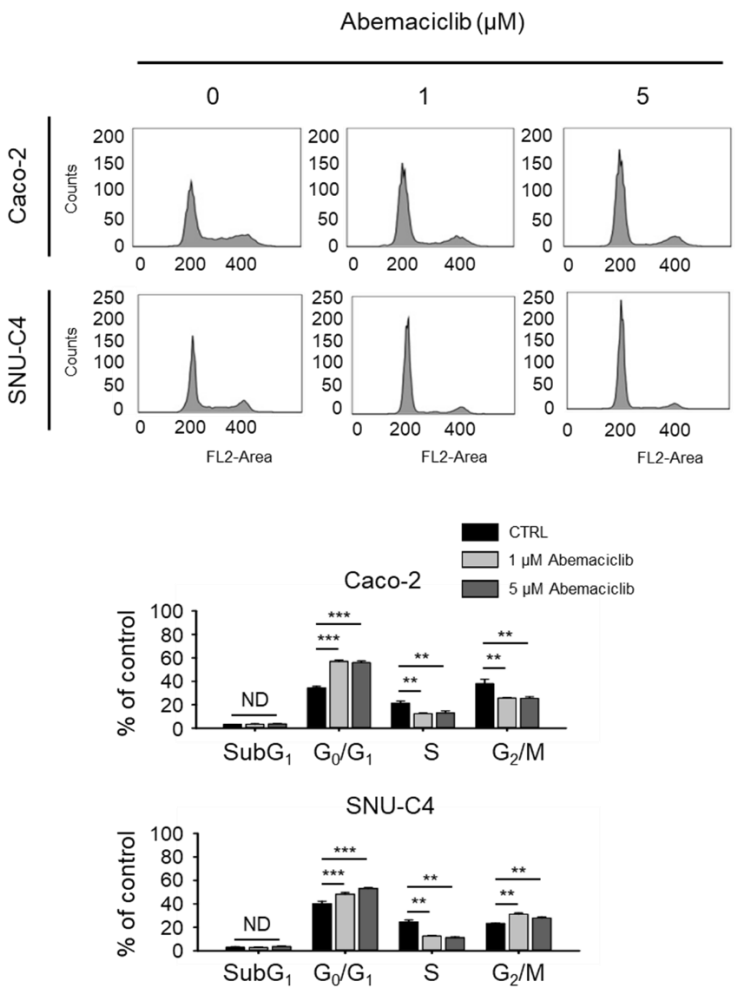

Figure 4. Changes of expression levels of cell cycle proteins during abemaciclib treatment

Expression levels of p-Rb, p130, p107, E2F, cyclin D1, cyclin E (lower band), and CDK2 were determined by western blot. GAPDH was used as a protein-loading control.

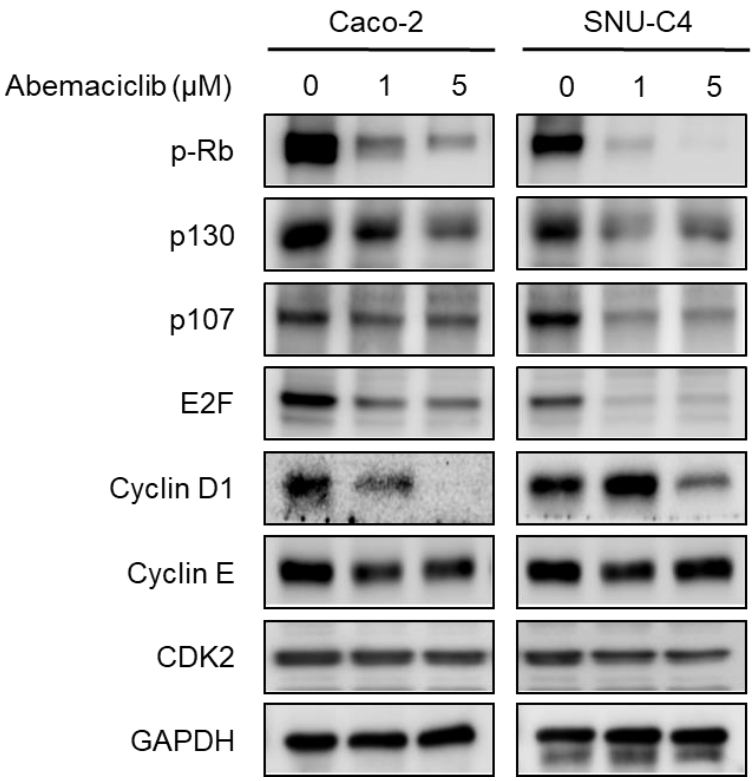

Figure 5. Colony-forming assay in abemaciclib sensitive cell lines

Colony-forming assays were conducted in Caco-2 and SNU-C4 cells. A total of 5×10^3 cells was seeded into 6-well plates and treated with abemaciclib for 7 days. Colony area was quantified using ImageJ software (National Institutes of Health, Bethesda, MD, USA). Data are expressed as the mean ± S.D. Different letters (a, b, c, d) indicate significant differences ($p < 0.05$).

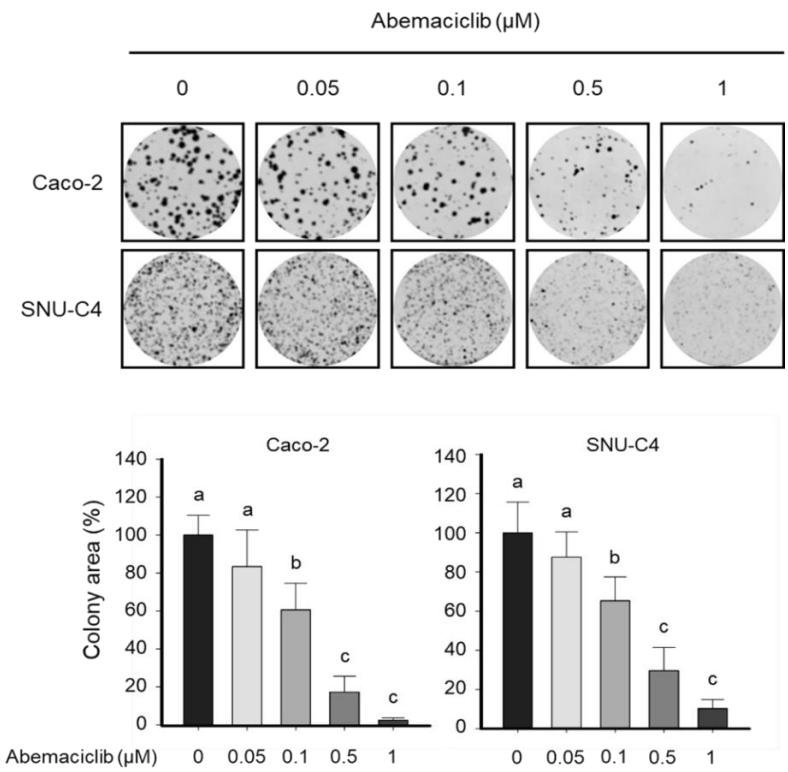

Abemaciclib and BYL719 combination shows synergistic anti-proliferative activity in *PIK3CA* mutated cell lines

Primary resistance cell lines against abemaciclib (HCT-15 and DLD-1) and abemaciclib sensitive cell lines (HT-29, Caco-2 and SNU-C4) were treated with 5 μM abemaciclib for 0, 5, 15, 30, 45, and 60 min. Western blot analysis of HT-29, Caco-2 and SNU-C4 cells displayed increased AKT phosphorylation by exposure to abemaciclib in a time-dependent manner **(Figure 6)**. Delayed tuberous sclerosis complex 2 (TSC2) phosphorylation was also observed in HT-29, Caco-2, and SNU-C4 cells with abemaciclib treatment. However, this was not evident in HCT-15 and DLD-1 cells.

Figure 6. Changes in AKT phosphorylation by exposure to abemaciclib

HCT-15, DLD-1, HT-29, Caco-2, and SNU-C4 cells were treated with 5 μM abemaciclib for 0, 5, 15, 30, 45, and 60 min. Expression levels of p-AKT S473, p-AKT T308, total AKT, p-TSC2, and total TSC2 were determined by Western blot. GAPDH was used as a protein-loading control.

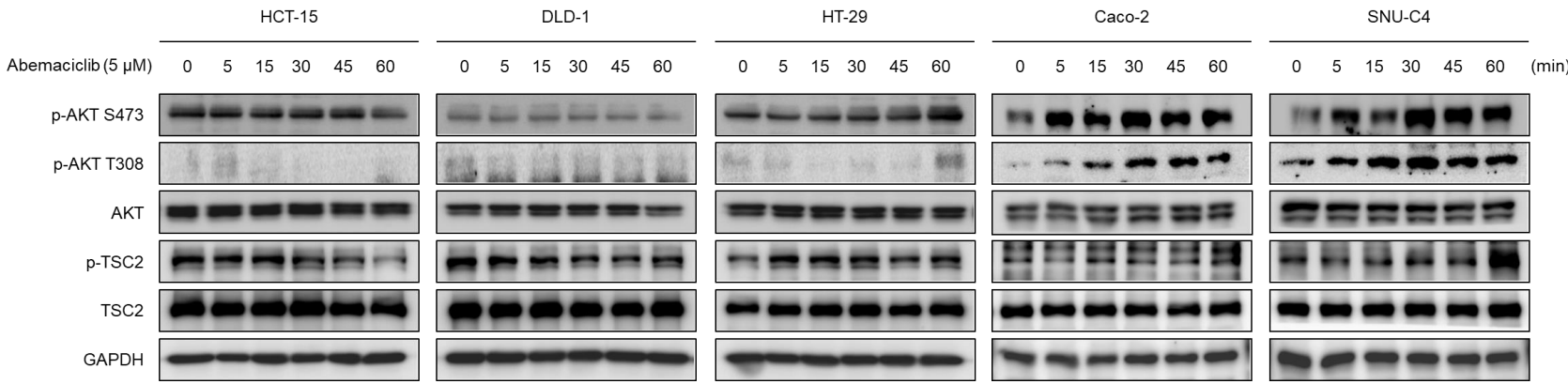

To find the optimal agent for overcoming the CDK4/6 inhibitor-resistance mechanism, several PI3K-AKT inhibitors, including AZD8186, ipatasertib, buparlisib, AZD5363, MK2206, and BYL719, were tested. Dose responses for these PI3K-AKT pathway inhibitors were characterized in HCT-15, DLD-1, HT-29, Caco-2 and SNU-C4 cells **(Figure 7)**. BYL719 was selected as a combination agent with abemaciclib against HT-29, Caco-2 and SNU-C4 cell survival to identify the effect of selective PI3K p110α inhibition according to the *PIK3CA* mutation status of the CRC cell lines.

Figure 7. IC_{50} concentrations of PI3K-AKT inhibitors in colorectal cancer cell lines

HCT-15, DLD-1, HT-29, Caco-2, and SNU-C4 cells were treated with the indicated concentrations of AZD8186, ipatasertib, buparlisib, AZD5363, MK2206, and BYL719 for 72 h.

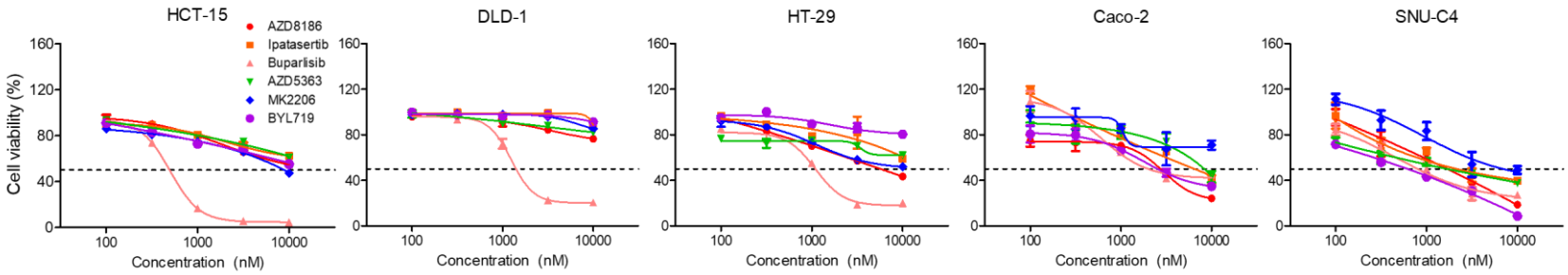

Abemaciclib/BYL719 combination treatment was effective in HT-29, Caco-2 and SNU-C4 cells and showed additive anti-proliferative activity in *PIK3CA* mutated HT-29 and SNU-C4 cells. In addition, we observed that 5μM of abemaciclib and 5μM of BYL719 combination treatment showed approximately two fold less toxic in normal colon epithelial CCD841CoN cell line compared with HT-29, Caco-2, and SNU-C4 cell lines **(Figure 8)**. Chou and Talalay multiple drug interaction analysis revealed further increased anti-proliferative effect of abemaciclib/BYL719 in HT-29 (CI=0.335, Fa<0.5), Caco-2 (CI = 0.447, Fa < 0.5) and SNU-C4 (CI = 0.286, Fa < 0.5) cells **(Figure 9 and Table 3)**.

Figure 8. Abemaciclib/BYL719 combination treatment in colorectal cancer cells and normal colon epithelial cell

HT-29, Caco-2, SNU-C4, and CCD840CoN cells were treated with 0, 1, and 5 μM abemaciclib and/or 0, 1, and 5 μM BYL719 for 72 h. Data represent the mean ± S.D. Different letters (a,b,c,d,e, and f) indicate significant differences ($p < 0.05$)

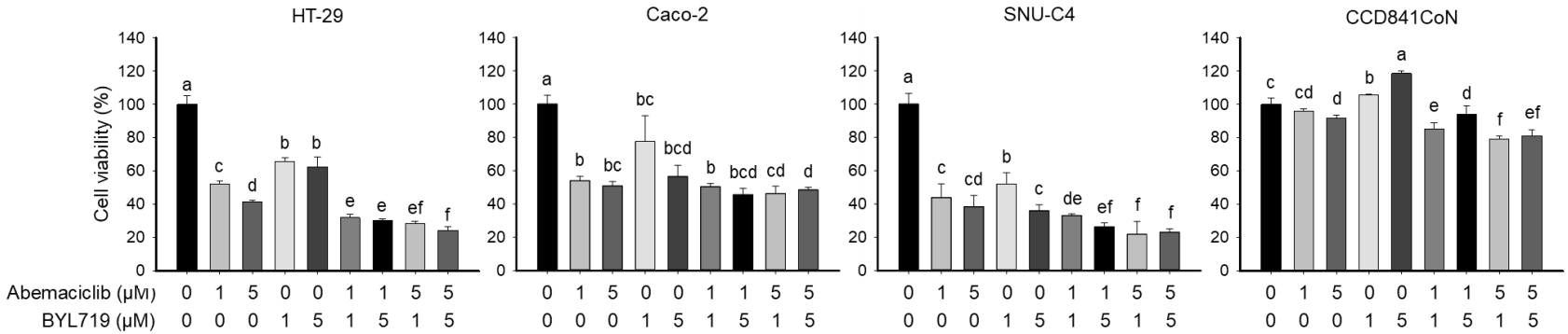

Figure 9. Chou and Talalay multiple drug interaction analysis in colorectal cancer cell lines

HT-29, Caco-2, and SNU-C4 cells were exposed to increasing concentrations of abemaciclib and BYL719 at a fixed ratio. The anti-proliferative potential of abemaciclib combined with BYL719 was determined by calculating the combination index (CI) using CalcuSyn software according to the Chou-Talalay method.

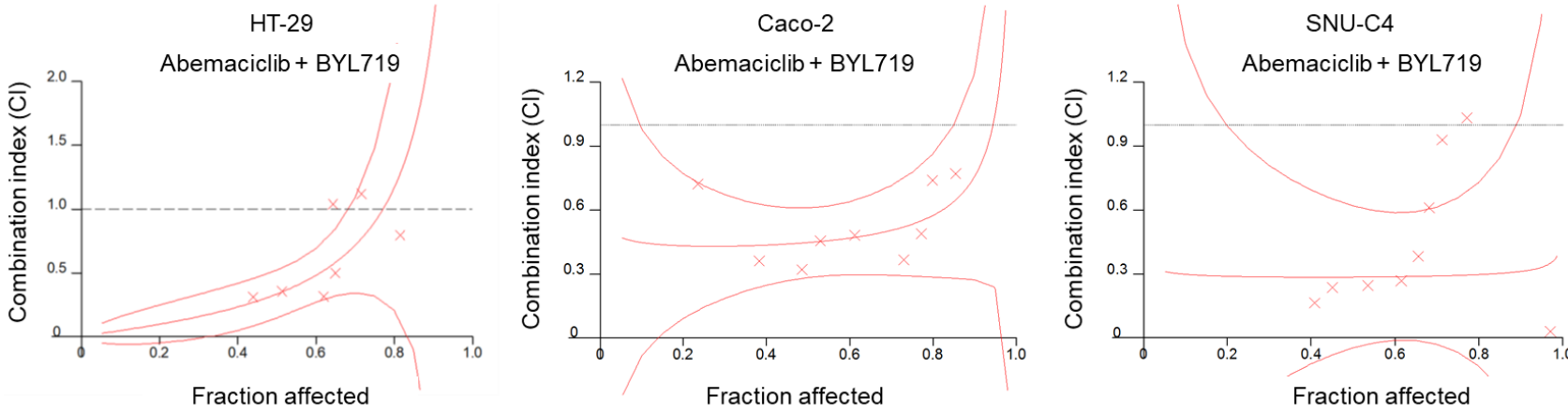

Table 3. Chou and Talalay multiple drug interaction analysis in colorectal cancer cell lines

HT-29					Caco-2					SNU-C4				
Fa	CI	Est. S.D.	Abemaciclib (µM)	BYL719 (µM)	Fa	CI	Est. S.D.	Abemaciclib (µM)	BYL719 (µM)	Fa	CI	Est. S.D.	Abemaciclib (µM)	BYL719 (µM)
0.02	0.011	0.025	2E-06	1E-05	0.02	0.513	0.579	2E-04	9E-04	0.02	0.336	1.306	2E-04	2E-04
0.05	0.025	0.04	3E-05	2E-04	0.05	0.472	0.387	0.001	0.006	0.05	0.313	0.805	0.001	0.001
0.1	0.048	0.057	3E-04	0.001	0.1	0.447	0.271	0.005	0.026	0.1	0.299	0.549	0.005	0.005
0.15	0.072	0.068	9E-04	0.004	0.15	0.437	0.212	0.012	0.065	0.15	0.293	0.432	0.013	0.011
0.2	0.098	0.077	0.002	0.012	0.2	0.432	0.173	0.024	0.131	0.2	0.29	0.359	0.026	0.022
0.25	0.127	0.084	0.005	0.026	0.25	0.429	0.145	0.043	0.233	0.25	0.288	0.307	0.045	0.038
0.3	0.158	0.089	0.01	0.051	0.3	0.43	0.124	0.072	0.385	0.3	0.287	0.267	0.073	0.062
0.35	0.193	0.092	0.019	0.096	0.35	0.432	0.108	0.113	0.608	0.35	0.286	0.235	0.113	0.096
0.4	0.234	0.094	0.035	0.174	0.4	0.435	0.096	0.174	0.933	0.4	0.286	0.209	0.17	0.145
0.45	0.28	0.095	0.061	0.306	0.45	0.44	0.088	0.261	1.405	0.45	0.286	0.187	0.252	0.215
0.5	0.335	0.096	0.107	0.533	0.5	0.447	0.083	0.39	2.099	0.5	0.286	0.171	0.371	0.316
0.55	0.401	0.098	0.186	0.928	0.55	0.457	0.083	0.583	3.135	0.55	0.287	0.159	0.545	0.464
0.6	0.482	0.108	0.327	1.634	0.6	0.469	0.087	0.879	4.722	0.6	0.288	0.153	0.807	0.687
0.65	0.583	0.134	0.59	2.948	0.65	0.484	0.095	1.347	7.239	0.65	0.289	0.155	1.215	1.035
0.7	0.716	0.19	1.108	5.539	0.7	0.505	0.107	2.126	11.43	0.7	0.291	0.165	1.882	1.603
0.75	0.899	0.296	2.218	11.09	0.75	0.534	0.124	3.515	18.89	0.75	0.294	0.185	3.047	2.596
0.8	1.166	0.489	4.912	24.56	0.8	0.575	0.147	6.248	33.59	0.8	0.298	0.22	5.29	4.506
0.85	1.602	0.873	12.86	64.29	0.85	0.639	0.183	12.54	67.41	0.85	0.304	0.276	10.31	8.787
0.9	2.447	1.792	46.16	230.8	0.9	0.756	0.246	31.64	170	0.9	0.313	0.372	25.04	21.33
0.95	4.888	5.312	363.8	1819	0.95	1.051	0.415	141	758	0.95	0.332	0.593	104.9	89.39
0.99	23.37	51.85	34787	2E+05	0.99	2.614	1.54	3830	20584	0.99	0.395	1.572	2486	2117

Abemaciclib and BYL719 combination induces G_0/G_1 phase arrest and alters regulatory protein expression in Caco-2 and SNU-C4 cell lines

Cell cycle analysis was performed to confirm the effects of abemaciclib and BYL719 on the cell cycle in Caco-2 and SNU-C4 cells **(Figure 10)**. Abemaciclib monotherapy induced G_0/G_1 arrest in Caco-2 and SNU-C4 cells. Abemaciclib/BYL719 combination also showed cell cycle arrest in the G_0/G_1 phase, but BYL719 monotherapy did not induce cell cycle arrest.

Figure 10. Abemaciclib and BYL719 combination inhibits the cell cycle in Caco-2 and SNU-C4 cell lines

A total of 1 × 10^6 cells was seeded in 60-mm plates and treated with the indicated concentrations of abemaciclib and BYL719 (n = 3). Bar graph shows the quantification of cell cycle distribution in Caco-2 and SNU-C4 cells. (Black, 0 μM abemaciclib and 0 μM BYL719; gray, 5 μM abemaciclib and 0 μM BYL719; dark gray, 0 μM abemaciclib and 5 μM BYL7190; light gray, 5 μM abemaciclib and 5 μM BYL719). ND no difference; *$p < 0.05$; **$p < 0.01$; and ***$p < 0.001$.

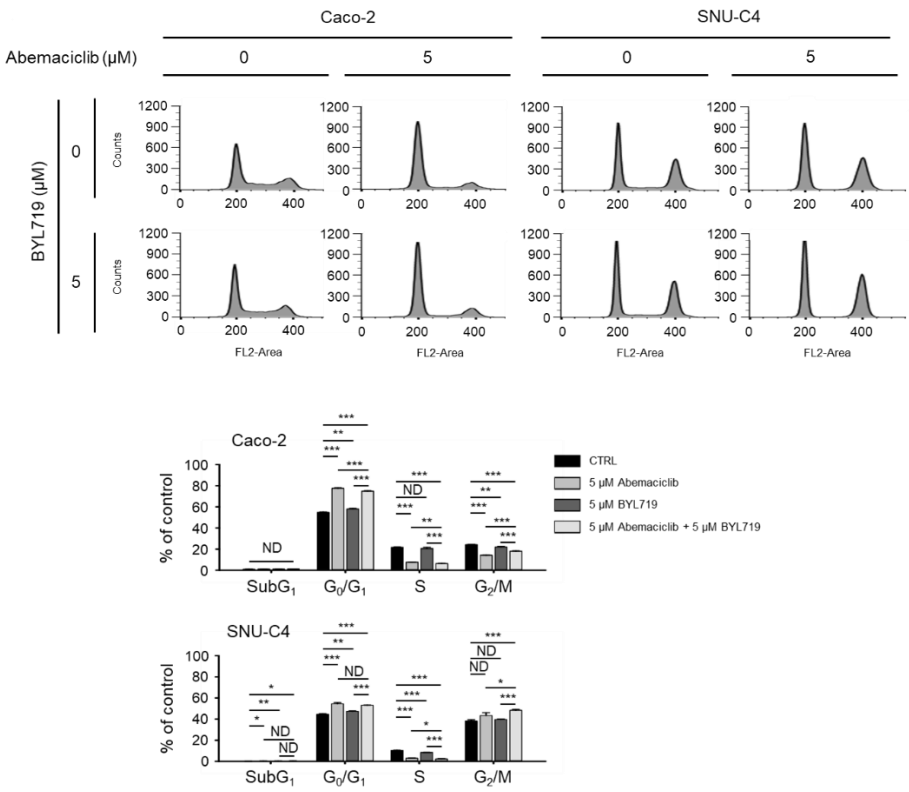

Changes in the protein expression levels of cell cycle regulators were evaluated in Caco-2 and SNU-C4 cells according to abemaciclib and BYL719 treatment **(Figure 11)**. Abemaciclib monotherapy decreased the expression of phosphorylated Rb (p-Rb), Rb, E2F, and cyclin A in Caco-2 and SNU-C4 cells. Rb phosphorylation was transiently inhibited with abemaciclib treatment in Caco-2 and SNU-C4 cells, but prolonged exposure (48 h) to abemaciclib monotherapy increased Rb phosphorylation in SNU-C4 cells. BYL719 alone did not affect p-Rb expression in both cell lines. Abemaciclib/BYL719 combination decreased the protein expression of p-Rb, and this effect was sustained longer compared with abemaciclib monotherapy. Sustained expression of cyclin D1, cyclin E, and CDK2 after abemaciclib monotherapy was also observed in this study. Cyclin A, cyclin E, and cyclin D1 were downregulated with abemaciclib/BYL719 combination in Caco-2 and SNU-C4 cells. CDK2 expression was not affected by any treatment in both cell lines.

Figure 11. Abemaciclib and BYL719 combination changes the expression of cell cycle regulatory proteins in Caco-2 and SNU-C4 cell lines

The expression levels of p-Rb, Rb, E2F, p16, cyclin A, cyclin E (lower band), cyclin D1, and CDK2 were evaluated by western blot using vinculin as a protein-loading control.

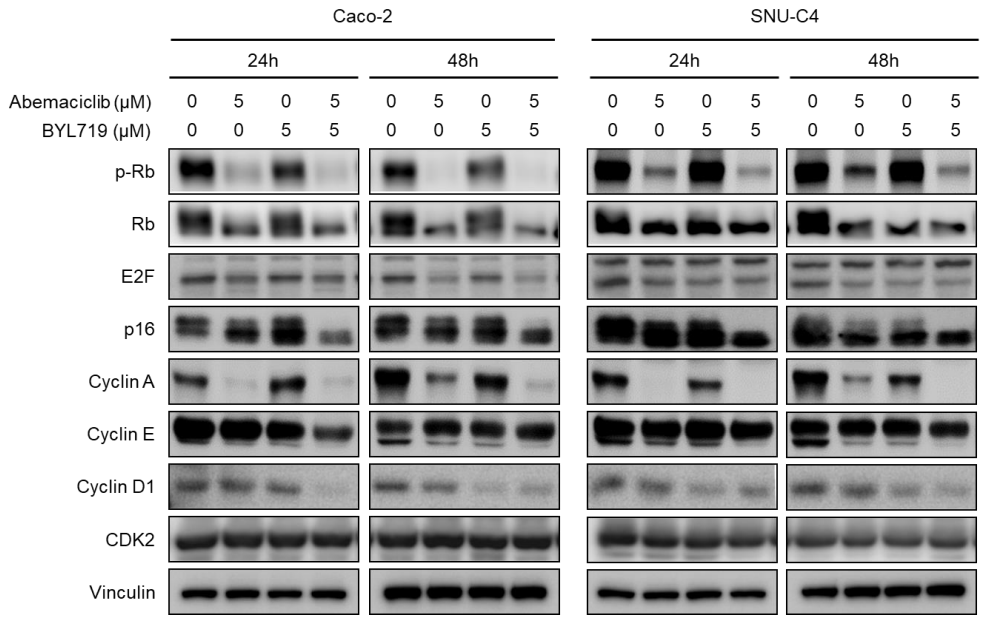

Abemaciclib and BYL719 combination inhibits colony-forming activity and cell migration

We performed colony-forming assays to determine whether abemaciclib/BYL719 combination could enhance the anti-proliferative activity in Caco-2 and SNU-C4 cells compared with abemaciclib and BYL719 monotherapy **(Figure 12)**. In both Caco-2 and SNU-C4 cells, abemaciclib and BYL719 monotherapies significantly suppressed colony-forming activity, whereas abemaciclib/BYL719 combination synergistically increased the inhibitory effects of abemaciclib and BYL719 alone in a dose-dependent manner.

Figure 12. Combination effects of abemaciclib and BYL719 on colony formation in Caco-2 and SNU-C4 cell lines

Colony-forming assays were conducted in Caco-2 and SNU-C4 cells treated with 0, 0.05, and 0.1 μM abemaciclib and/or 0, 1, and 5 μM BYL719 for 10 days.

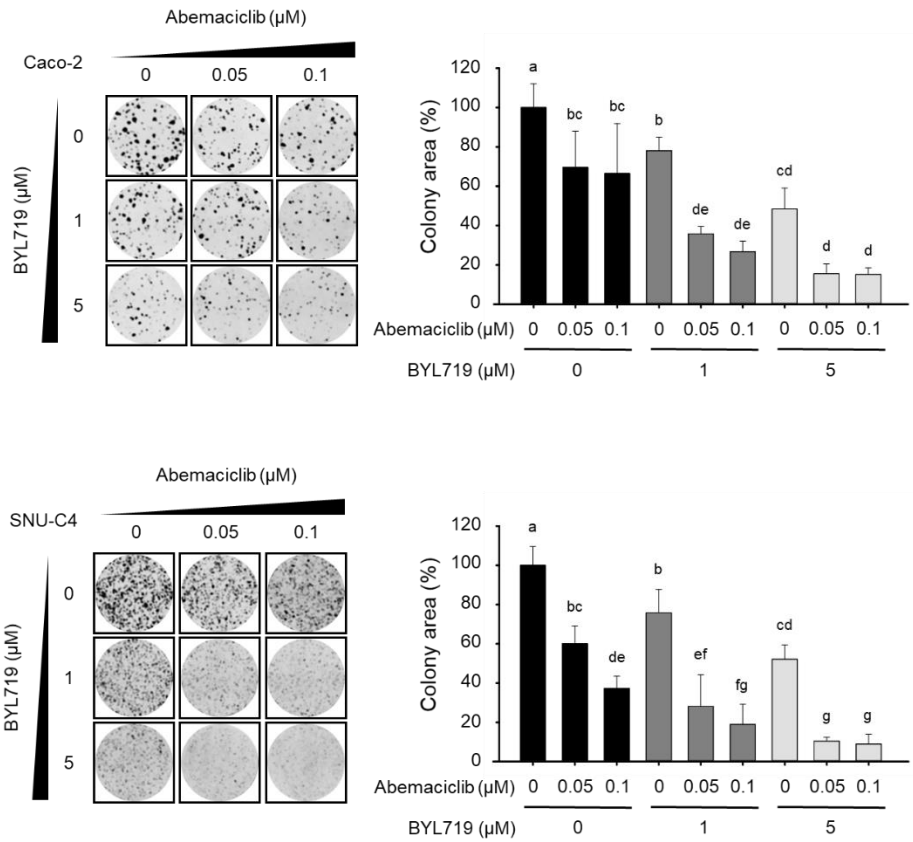

The effect of abemaciclib/BYL719 combination on migration was evaluated using a scratch wound healing assay **(Figure 13)**. Although abemaciclib monotherapy significantly inhibited cell migration in Caco-2 cells, BYL719 monotherapy and abemaciclib/BYL719 combination did not inhibit cell migration. In contrast, although abemaciclib alone was insufficient to alter the migration ability of SNU-C4 cells below 5 μM, abemaciclib/BYL719 combination and BYL719 monotherapy resulted in potent migration inhibition in SNU-C4 cells.

Figure 13. Combination effects of abemaciclib and BYL719 on migration in Caco-2 and SNU-C4 cell lines

The migration of Caco-2 and SNU-C4 cells was assessed by wound healing assays after 40 h of treatment. Representative images of the scratched areas are shown. Cell migration was quantified using ImageJ software.

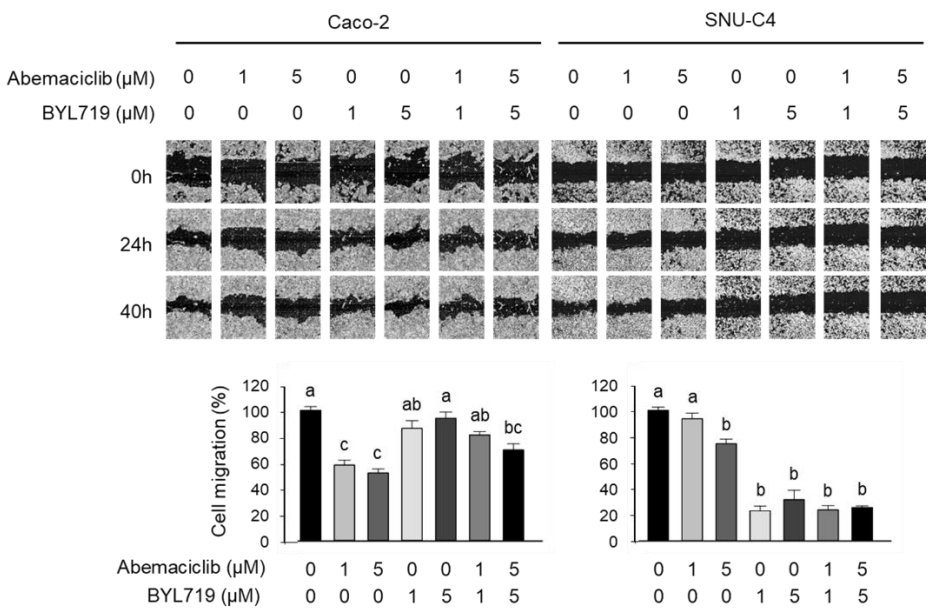

Abemaciclib and BYL719 combination inhibits tumor growth and induces apoptosis *in vivo*

SNU-C4 cells showed a more potent synergistic response when treated with abemaciclib/BYL719 combination than Caco-2 cells **(Figure 10, 11, 12, 13)**. Using a mouse xenograft model of SNU-C4 cells, the *in vivo* anti-tumor activity of abemaciclib/BYL719 combination was evaluated. Mice were randomly assigned to receive one of the following treatments: (A) three times weekly oral administration of vehicle, i.e., sterile water (control group, n=5), (B) daily oral administration of abemaciclib (25 mg/kg/day of body weight) in sterile water (n=5), (C) daily oral administration of abemaciclib (50 mg/kg/day of body weight) in sterile water (n=5), (D) daily oral administration of BYL719 (15 mg/kg/day of body weight) in sterile water (n=5), (E) daily oral administration of BYL719 (30 mg/kg/day of body weight) in sterile water (n=5), (F) daily oral administration of abemaciclib (25 mg/kg/day of body weight) combined with BYL719 (15 mg/kg/day of body weight) in sterile water (n=5), or (G) daily oral administration of abemaciclib (50 mg/kg/day of body weight) combined with BYL719 (30 mg/kg/day of body weight) in sterile water (n=5). During the 4 weeks of treatment, there was no significant change in body weight among the seven treatment groups **(Figure 14A)**. However, three deaths were reported in group G at week 3 **(Figure 14B)**, whereas there were no deaths in the other groups.

Figure 14. Tolerability of abemaciclib combined with BYL719 in SNU-C4 mouse xenograft models

Athymic nude mice bearing SNU-C4 xenografts were administered with vehicle, abemaciclib alone, BYL719 alone, or the combination of abemaciclib and BYL719.

(A) Body weight were evaluated every 7 days.

(B) Survival data of mice were evaluated every 7 days.

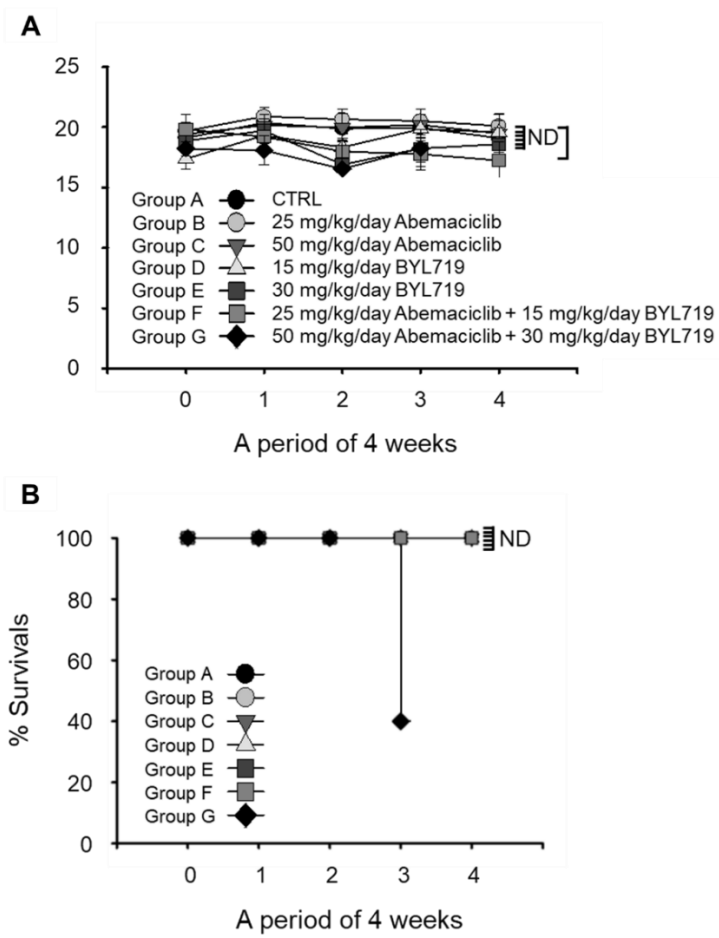

The volume of tumors in the control group increased during the follow-up **(Figure 15)**. Abemaciclib or BYL719 monotherapy significantly inhibited tumor growth compared with the control group ($p < 0.05$). Abemaciclib/BYL719 combination showed a more potent inhibitory growth effect compared with the abemaciclib or BYL719 monotherapy groups ($p < 0.05$).

Figure 15. The overall anti-tumor efficacy of treatment regimens in SNU-C4 mouse xenograft models

The overall anti-tumor efficacy of drugs was measured by tumor volume every 7 days. Error bars represent the standard error of the mean.

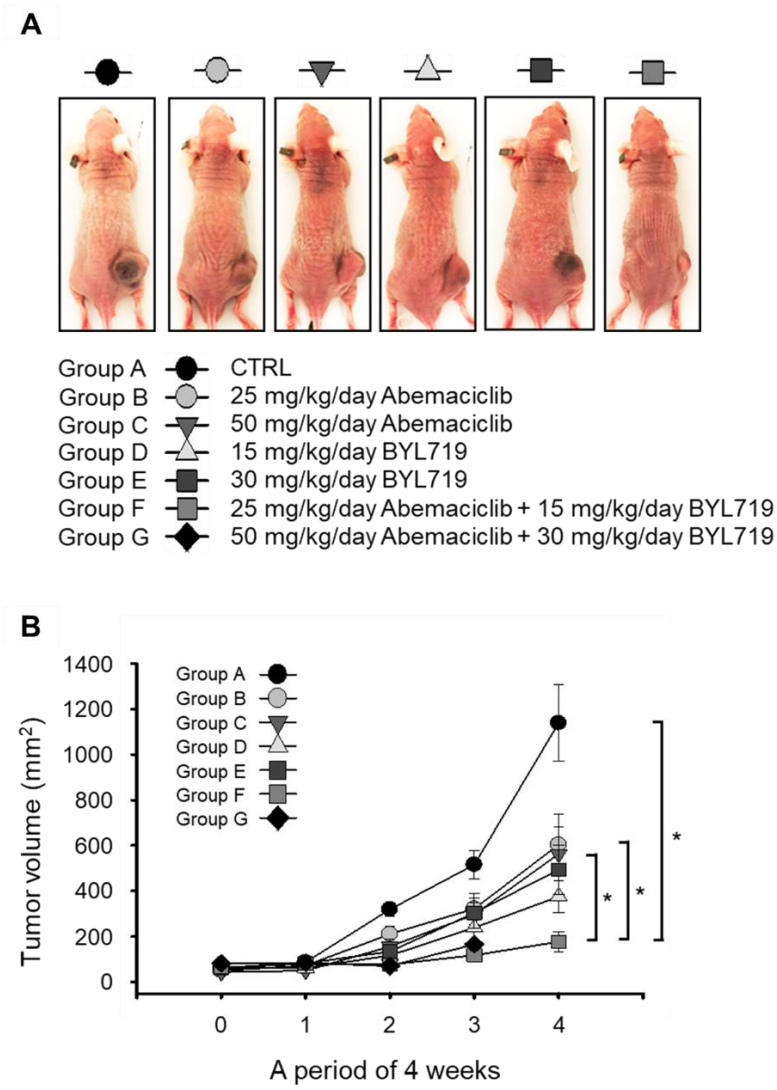

Formalin-fixed paraffin-embedded tumor tissues from the SNU-C4 mouse xenograft model were stained with H&E and for p-AKT S473, Ki67, and TUNEL assay **(Figure 16)**. Ki67 expression dramatically decreased in the combination groups, indicating less cell proliferation, compared with the control and monotherapy groups **(Figure 17)**. In the abemaciclib and BYL719 monotherapy groups, there was only a slight increase in the amount of TUNEL-positive cells, suggesting apoptosis, at high doses (30 mg/kg/day) of BYL719 monotherapy compared with the control group. However, abemaciclib/BYL719 combination treatment appeared to increase TUNEL-positive cells compared with abemaciclib or BYL719 monotherapies **(Figure 18)**.

Figure 16. Tumor sections from the SNU-C4 mouse xenograft model (x100)

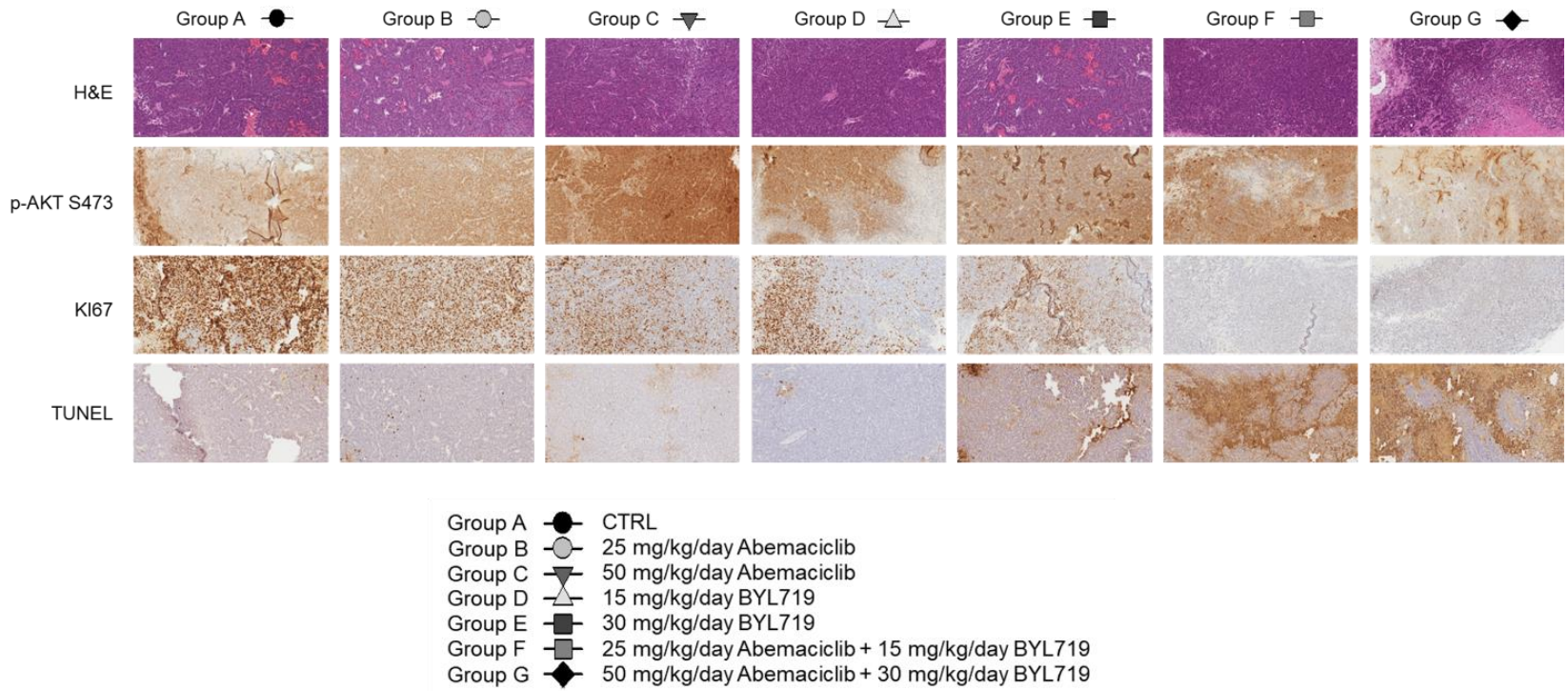

Figure 17. Ki-67 expression of tumor tissues from the SNU-C4 mouse xenograft model (x400)

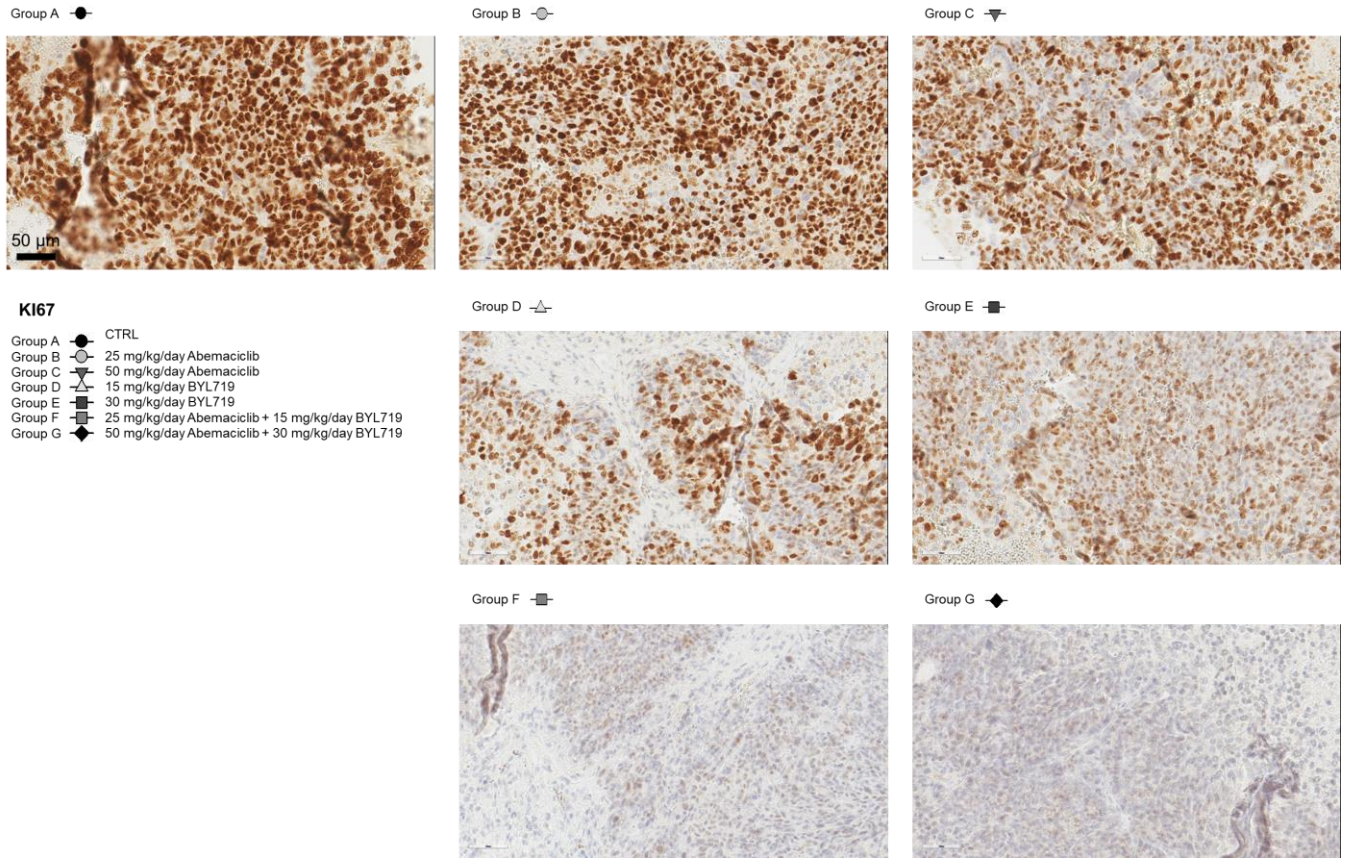

Figure 18. TUNEL staining of tumor tissues from the SNU-C4 mouse xenograft model (x400)

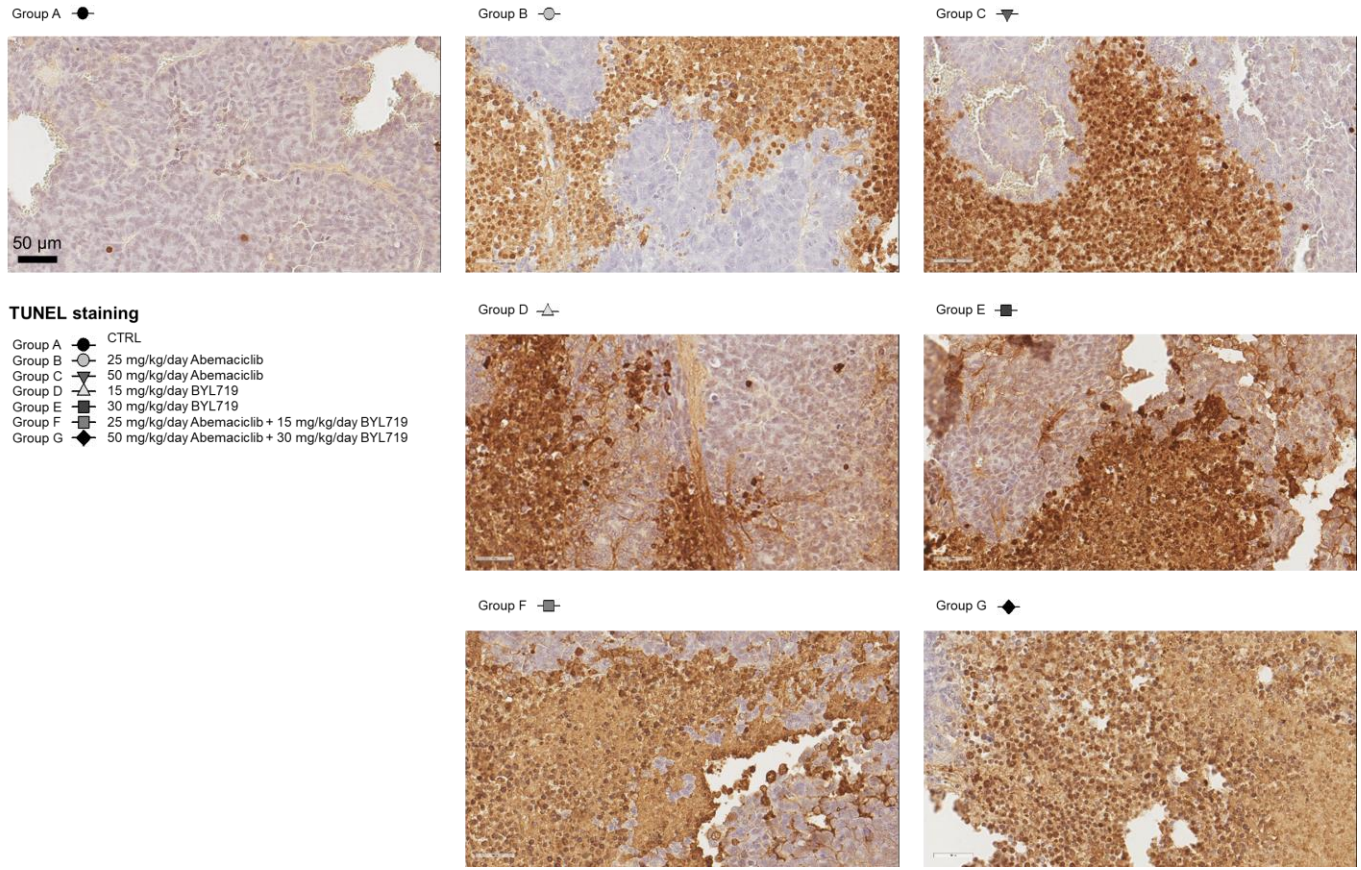

Discussion

This study demonstrates that abemaciclib monotherapy induces cell cycle arrest and inhibits cell proliferation in CRC cell lines. Furthermore, abemaciclib has a synergistic effect in combination with BYL719 both in *in vivo* and *in vitro* CRC cell line models. This synergistic effect was more significantly demonstrated in the *PIK3CA* mutated cell line than in the *PIK3CA* wild-type cell line. We also found that cell cycle arrest, proliferation and migration inhibition, and apoptosis contributed to the anti-tumor activity of abemaciclib/BYL719 combination therapy in the *PIK3CA* mutated CRC cells.

Previous studies using different selective CDK4/6 inhibitors reported that abemaciclib (IC_{50} 2 nM) is the most potent selective CDK4/6 inhibitor against the cyclin D1/CDK4 complex and palbociclib (IC_{50} 11 nM) showed similar potency with ribociclib (IC_{50} 9 nM) against the cyclin D1/CDK4 complex [17]. Abemaciclib is the most recently developed selective CDK4/6 inhibitor with distinct characteristics from other selective CDK4/6 inhibitors, such as palbociclib and ribociclib. Abemaciclib has shown superior single-agent activity when compared with palbociclib and ribociclib [18-20], and it is more selective against CDK4 than CDK6 compared with other CDK4/6 inhibitors [21]. Consequently, abemaciclib has shown higher clinical activity while reducing the episodes of severe neutropenia that result from CDK6 inhibition [22]. Less frequent neutropenia allows continuous dosing of abemaciclib to achieve durable cell cycle inhibition, and continuous exposure to higher plasma concentrations

of abemaciclib is a key mechanism for inducing apoptosis in preclinical models [23]. In our study with CRC cell lines, abemaciclib was the most effective (mean GI_{50} 2.05 μM) of the selective CDK4/6 inhibitors tested, followed by palbociclib (mean GI_{50} 4.14 μM) and ribociclib (mean GI_{50} 17.77 μM). Cell lines with IC_{50} below 1 μM are defined to represent sensitive cell lines to palbociclib and ribociclib according to previous preclinical studies [24,25]. Gong, et al. reasoned that IC_{50} below 1 μM represent the clinically available dose that tumors could be responsive to abemaciclib monotherapy [7]. Based on these previous literatures, we decided the sensitivity cut-off of all selective CDK4/6 inhibitors' concentration as GI_{50} concentrations <1 μM. The limitation of our study is a concurrent use GI_{50} and IC_{50} values in the process of confirming the effect of the drug. In the initial stage of this study, we hypothesize that the main mechanism of anti-tumor activity of abemaciclib would be growth inhibition like any other previously developed CDK4/6 inhibitors. As a result, GI_{50} was used for confirming antitumor activity of abemaciclib in CRC cell lines. In the course of our study, we realized that abemaciclib exerts the anti-tumor activity beyond enforcing cytostatic growth arrest. Thus, we have performed cell viability test and calculate IC_{50} to analyze the anti-tumor activity of molecular-targeted agents and abemaciclib combination treatment. Abemaciclib demonstrated relatively potent growth inhibitory activity with the lowest mean GI_{50} concentration whereas the most of the CRC cell lines were resistant to ribociclib. As a result, abemaciclib was selected to explore the efficacy and mechanism of action in CRC cell lines in further experiments.

In our study, abemaciclib-sensitive CRC cell lines presented some common features, including *KRAS* wild-type, intact Rb expression, low p16 expression, and relatively low cyclin D1 expression. An early phase clinical trial with abemaciclib had reported that disease control rate for the *KRAS* mutant population was 55% (16 of 29 patients), whereas that for the *KRAS* wild-type population was 39% (13 of 33 patients) especially in non-small cell lung cancer (NSCLC) cohort [26]. However, this result did not translate into late stage clinical trial. A phase III trial with abemaciclib monotherapy in *KRAS*-mutated, NSCLC did not meet its primary endpoint of OS [27]. *KRAS* mutation are reported in 50% of CRC [28] and still remains a challenging target that has no effective therapeutic option in many human cancers. *KRAS* mutation status as a single predictive marker for selective CDK4/6 inhibitors in CRC have not been reported yet and need to be further validated in other preclinical and clinical trials. Various clinical and preclinical studies have demonstrated that Rb could be the most important predictive marker for CDK4/6 inhibitors [29-31]. Consistent with these reports, our study showed that intact Rb is a sensitivity biomarker for CDK4/6 inhibitors. However, a recent study, which assessed abemaciclib sensitivity across many human cancer cell lines, suggested that loss of p16 and low cyclin D1 expression were associated with abemaciclib resistance [7]. Among these markers, the role of cyclin D1 and p16 expression as prognostic markers for CDK4/6 inhibitors is still controversial, even in similar groups of patients with ER+/HER2- breast cancer [32,33], and requires further evaluation in preclinical and clinical models.

CDK2 and its regulatory cyclin-cyclin E are also known as another key factors in the progression of cell cycle transition from G1 to S phase as well

as CDK4/6-cyclin D1 complex [34]. In addition, it was previously reported that PI3K/AKT/mTOR signaling pathway activation promotes cell cycle progression in CDK4/6 inhibitor resistant breast cancer cells through increased CDK2 and cyclin E [35]. Sustained expression of cyclin E, and CDK2 **(Figure 11)** after abemaciclib monotherapy was observed in our study. This might result in delayed Rb phosphorylation in abemaciclib monotherapy. However, Rb phosphorylation and cyclin E expression decreased with abemaciclib/BYL719 combination therapy in our study. These findings suggest that CDK4/6-independent signaling pathways, which could be blocked by BYL719 combination treatment, could exist in CRC cell lines like breast cancer cell lines. In a preclinical study by Herrera-Abreu, et al., elevated cyclin E expression and failed inhibition of Rb phosphorylation were detected in *PIK3CA* mutated breast cancer cell lines [36]. Prolonged CDK4/6 single inhibition and PI3K and CDK4/6 dual inhibition resulted in loss of Rb phosphorylation and reduced cyclin E expression in the same study [36]. Our study with CRC cell lines suggested that CDK2-mediated Rb phosphorylation in combination with cyclin E expression could be a mechanism of resistance to CDK4/6 inhibition.

AKT phosphorylation **(Figure 6)** after abemaciclib monotherapy was also observed in this study. AKT phosphorylation is known as a potential acquired resistance mechanism for CDK4/6 inhibitors [35]. This finding indicated that activated AKT signaling by abemaciclib could be an acquired resistance mechanism against abemaciclib treatment, which could be blocked by combination therapy with PI3K-AKT signaling inhibitors. PI3K/AKT/mTOR signaling pathway activation via AKT phosphorylation is a well-known resistance mechanism against CDK4/6 inhibitors [35-37]. The

PI3K/AKT/mTOR pathway is activated in many kinds of cancers and the activation of PI3K/AKT/mTOR pathway is mainly mediated by mutations in the p110α subunit of PI3K called *PIK3CA* (>80%) [38]. *PIK3CA* mutations have been found in approximately 16–21% of CRC [39]. It was previously reported that CDK4/6 inhibitors activated the PI3K/AKT pathway through the phosphorylation of S473/T308 on AKT, and CDK4/6 and PI3K inhibitor combination reduced AKT phosphorylation in *PIK3CA* mutated breast cancer cell lines. In the same study, PI3K inhibition downregulated cyclin D1 expression [24]. These findings are consistent with our findings in CRC cell lines and suggest that PI3K inhibition in combination with CDK4/6 inhibition might have the potential to overcome resistance to CDK4/6 inhibitors.

Some preclinical and early clinical studies have suggested the potential efficacy of *PIK3CA*-targeting agents [40]; however, the clinical applications of PI3K inhibitors have not advanced to late-phase clinical trials due to the lack of rationale for combination strategies and toxicities. Isoform-specific PI3K inhibitors are expected to have a wider range of therapeutic index and less off-target effects, resulting in lower toxicity. BYL719 is a selective PI3K p110α inhibitor with potent activity against its activation [41]. In our data, abemaciclib and BYL719 combination showed different outcomes according to the *PIK3CA* mutation status in each CRC cell line. SNU-C4 cells harbor the *PIK3CA* mutation, whereas Caco-2 cells do not harbor any actionable mutations in the same gene. Iida et al. reported that CDK4/6 inhibitor-resistant breast cancer cell lines were more dependent on the PI3K/AKT/mTOR pathway [42]. Almost all of the CRC cell lines used in our study were more resistant to abemaciclib (GI_{50} > 1.0 μM) compared with

breast cancer cell lines (mean IC_{50} = 168 nM) [43]. CDK4/6 inhibitors limit cell proliferation by decreasing Rb phosphorylation, but inhibiting Rb phosphorylation with CDK4/6 inhibitors leads to mammalian target of rapamycin complex 2 (mTORC2)-mediated AKT activation in Rb-proficient cells [44]. Delayed AKT and TSC2 phosphorylation with abemaciclib treatment was observed in SNU-C4 cells in our study **(Figure 6)**. These findings support the hypothesis that there can be complex crosstalk between cell cycle and mitogenic signaling pathways in CRC cells, and that *PIK3CA* mutated CRC cells might be more dependent on the PI3K/AKT/mTOR pathway than breast cancer cells.

Among the multiple PI3K-AKT inhibitors tested in our study, BYL719 showed potent anti-proliferative efficacy against Caco-2 and SNU-C4 cells, which was more prominent in the SNU-C4 cells. Interestingly, abemaciclib and BYL719 combination therapy significantly decreased colony-forming activity and migration in SNU-C4 cells but displayed antagonism in Caco-2 cell migration **(Figure 13)**. Therefore, we evaluated the *in vivo* efficacy of abemaciclib and BYL719 combination therapy using a mouse xenograft model of *PIK3CA* mutated SNU-C4 cells. The SNU-C4 tumor xenograft model revealed that combining abemaciclib and BYL719 could not only inhibit tumor growth **(Figure 15)**, but also induce apoptosis **(Figure 16-18)**. Abemaciclib has proven its cytostatic properties in various cancer types, but it sometimes exhibits cytotoxic properties alone or in combination with other agents [26,43]. *In vitro* data from our study gave rationale for abemaciclib and BYL719 combination therapy, and *in vivo* data with a *PIK3CA* mutated CRC mouse xenograft model confirmed the efficacy of abemaciclib and BYL719 combination therapy. Thus, it could be reasonable

to suggest that adding BLY719 with abemaciclib leads to durable anti-tumor effects in some tumor types with *PIK3CA* mutations.

Unfortunately, specific predictive markers for abemaciclib have yet to be discovered, except for Rb proficiency in some studies [45]. The single-agent activity of abemaciclib has resulted in limited outcomes in many clinical trials, so the focus of recent clinical trials with CDK4/6 inhibitors has moved to combination therapy and to find alternative predictive markers in response to combination therapy. There are some ongoing clinical trials to evaluate the safety and efficacy of CDK4/6 and PI3K/AKT dual inhibition. Palbociclib with PI3K/mTOR inhibitor PF-05212384 in patients with estrogen receptor positive (ER+) metastatic breast cancer (MBC) reported promising preliminary anti-tumor activity with manageable toxicities [46]. Palbociclib and PI3K inhibitor, taselisib, combination treatment in patients with *PIK3CA* mutated advanced breast cancer revealed clinical benefit with tolerable toxicities [47]. Aromatase inhibitor in combination with ribociclib and BYL719 demonstrated enhanced anti-tumor activity without evidence of drug interaction in patients with ER+ HER2 negative breast cancer [48]. Although there is a lack of clinical data for abemaciclib because of its short developmental history, abemaciclib and selective PI3K p110α inhibitor combination are expected to be promising in clinical use. In consistent with our data, abemaciclib and selective PI3K p110α inhibitor combination was superior to single agent treatment in patient-derived xenograft models with *PIK3CA* mutated head and neck squamous cell carcinoma [49]. Until now, there are few studies to explore the efficacy and feasibility of CDK4/6 inhibitors in combination with PI3K inhibitors in patients with CRC. Moreover, *KRAS* mutation status was not evaluated or stratified in most of

the previous studies to evaluate the anti-tumor activity of CDK4/6 and PI3K/AKT dual inhibition. Our study also did not demonstrate the effect of selective CDK4/6 and PI3K p110α dual inhibition in *KRAS* mutated CRC cell lines. The findings of our study propose that *PIK3CA* mutation could be a predictive marker for the response to abemaciclib and BYL719 combination therapy in colorectal cancer treatment, and it should be validated in further preclinical and clinical trials according to the *KRAS* mutational status.

In the present study, our findings suggest that abemaciclib and BYL719 combination therapy is effective in preclinical CRC cell line models. Cell cycle arrest, proliferation and migration inhibition, and apoptosis are the main contributors to the anti-tumor activity of abemaciclib and BYL719 combination therapy. Moreover, our study suggests that *PIK3CA* mutation could be an additional predictive marker for the efficacy of abemaciclib in combination with BYL719. These findings provide novel insight into a possible therapeutic strategy for patients with refractory metastatic CRC.

References

1. Jung, K.-W.; Won, Y.-J.; Kong, H.-J.; Lee, E.S. Cancer Statistics in Korea: Incidence, Mortality, Survival, and Prevalence in 2016. Cancer Res Treat 2019, 51, 417-430, doi:10.4143/crt.2019.138.

2. Bray, F.; Ferlay, J.; Soerjomataram, I.; Siegel, R.L.; Torre, L.A.; Jemal, A. Global cancer statistics 2018: GLOBOCAN estimates of incidence and mortality worldwide for 36 cancers in 185 countries. CA Cancer J Clin 2018, 68, 394-424, doi:10.3322/caac.21492.

3. Siegel, R.L.; Miller, K.D.; Jemal, A. Cancer statistics, 2015. CA Cancer J Clin 2015, 65, 5-29, doi:10.3322/caac.21254.

4. Classon, M.; Harlow, E. The retinoblastoma tumour suppressor in development and cancer. Nature Reviews Cancer 2002, 2, 910-917, doi:10.1038/nrc950.

5. Toncheva, D.; Petrova, D.; Tzenova, V.; Dimova, I.; Yankova, R.; Yordanov, V.; Damjanov, D.; Todorov, T.; Zaharieva, B. Tissue microarray analysis of cyclin D1 gene amplification and gain in colorectal carcinomas. Tumour Biol 2004, 25, 157-160, doi:10.1159/000081097.

6. McKay, J.A.; Douglas, J.J.; Ross, V.G.; Curran, S.; Murray, G.I.; Cassidy, J.; McLeod, H.L. Cyclin D1 protein expression and gene polymorphism in colorectal cancer. Aberdeen Colorectal Initiative. Int J Cancer 2000, 88, 77-81, doi:10.1002/1097-0215(20001001)88:1.

7. Gong, X.; Litchfield, L.M.; Webster, Y.; Chio, L.-C.; Wong, S.S.; Stewart, T.R.; Dowless, M.; Dempsey, J.; Zeng, Y.; Torres, R., et al. Genomic Aberrations that Activate D-type Cyclins Are Associated with Enhanced Sensitivity to the CDK4 and CDK6 Inhibitor Abemaciclib. Cancer Cell 2017, 32, 761-776.e766, doi:10.1016/j.ccell.2017.11.006.

8. Hanahan, D.; Weinberg, Robert A. Hallmarks of Cancer: The Next Generation. Cell 2011, 144, 646-674, doi:10.1016/j.cell.2011.02.013.

9. Filmus, J.; Robles, A.I.; Shi, W.; Wong, M.J.; Colombo, L.L.; Conti, C.J. Induction of cyclin D1 overexpression by activated ras. Oncogene 1994, 9, 3627-3633.

10. Boussios, S.; Ozturk, M.A.; Moschetta, M.; Karathanasi, A.; Zakynthinakis-Kyriakou, N.; Katsanos, K.H.; Christodoulou, D.K.; Pavlidis, N. The Developing Story of Predictive Biomarkers in Colorectal Cancer. J Pers Med 2019, 9, doi:10.3390/jpm9010012.

11. Yang, J.; Nie, J.; Ma, X.; Wei, Y.; Peng, Y.; Wei, X. Targeting PI3K in cancer: mechanisms and advances in clinical trials. Molecular Cancer 2019, 18, 26, doi:10.1186/s12943-019-0954-x.

12. Diehl, J.A.; Cheng, M.; Roussel, M.F.; Sherr, C.J. Glycogen synthase kinase-3beta regulates cyclin D1 proteolysis and subcellular localization. Genes Dev 1998, 12, 3499-3511, doi:10.1101/gad.12.22.3499.

13. Zacharek, S.J.; Xiong, Y.; Shumway, S.D. Negative Regulation of TSC1-TSC2 by Mammalian D-Type Cyclins. Cancer Research 2005, 65, 11354-11360, doi:10.1158/0008-5472.Can-05-2236.

14. Chou, T.C. Theoretical basis, experimental design, and computerized simulation of synergism and antagonism in drug combination studies. Pharmacol Rev 2006, 58, 621-681, doi:10.1124/pr.58.3.10.

15. Cancer Cell Line Encyclopedia. Availabe online: https://portals.broadinstitute.org/ccle (accessed on 4 Apr 2020).

16. Catalogue Of Somatic Mutations In Cancer (COSMIC). Availabe online: https://cancer.sanger.ac.uk/cosmic (accessed on 4 Apr 2020).

17. Klein, M.E.; Kovatcheva, M.; Davis, L.E.; Tap, W.D.; Koff, A. CDK4/6 Inhibitors: The Mechanism of Action May Not Be as Simple as Once Thought. Cancer Cell 2018, 34, 9-20, doi:10.1016/j.ccell.2018.03.023.

18. Dickler, M.N.; Tolaney, S.M.; Rugo, H.S.; Cortés, J.; Diéras, V.; Patt, D.; Wildiers, H.; Hudis, C.A.; O'Shaughnessy, J.; Zamora, E., et al. MONARCH 1, A Phase II Study of Abemaciclib, a CDK4 and CDK6 Inhibitor, as a Single Agent, in Patients with Refractory HR(+)/HER2(-) Metastatic Breast Cancer. Clin Cancer Res 2017, 23, 5218-5224, doi:10.1158/1078-0432.Ccr-17-0754.

19. DeMichele, A.; Clark, A.S.; Tan, K.S.; Heitjan, D.F.; Gramlich, K.; Gallagher, M.; Lal, P.; Feldman, M.; Zhang, P.; Colameco, C., et al. CDK 4/6 inhibitor palbociclib (PD0332991) in Rb+ advanced breast cancer: phase II activity, safety, and predictive biomarker assessment. Clin Cancer Res 2015, 21, 995-1001, doi:10.1158/1078-0432.Ccr-14-2258.

20. Infante, J.R.; Cassier, P.A.; Gerecitano, J.F.; Witteveen, P.O.; Chugh, R.; Ribrag, V.; Chakraborty, A.; Matano, A.; Dobson, J.R.; Crystal,

A.S., et al. A Phase I Study of the Cyclin-Dependent Kinase 4/6 Inhibitor Ribociclib (LEE011) in Patients with Advanced Solid Tumors and Lymphomas. Clin Cancer Res 2016, 22, 5696-5705, doi:10.1158/1078-0432.Ccr-16-1248.

21. Gelbert, L.M.; Cai, S.; Lin, X.; Sanchez-Martinez, C.; Del Prado, M.; Lallena, M.J.; Torres, R.; Ajamie, R.T.; Wishart, G.N.; Flack, R.S., et al. Preclinical characterization of the CDK4/6 inhibitor LY2835219: in-vivo cell cycle-dependent/independent anti-tumor activities alone/in combination with gemcitabine. Invest New Drugs 2014, 32, 825-837, doi:10.1007/s10637-014-0120-7.

22. Scheicher, R.; Hoelbl-Kovacic, A.; Bellutti, F.; Tigan, A.S.; Prchal-Murphy, M.; Heller, G.; Schneckenleithner, C.; Salazar-Roa, M.; Zöchbauer-Müller, S.; Zuber, J., et al. CDK6 as a key regulator of hematopoietic and leukemic stem cell activation. Blood 2015, 125, 90-101, doi:10.1182/blood-2014-06-584417.

23. Torres-Guzmán, R.; Calsina, B.; Hermoso, A.; Baquero, C.; Alvarez, B.; Amat, J.; McNulty, A.M.; Gong, X.; Boehnke, K.; Du, J., et al. Preclinical characterization of abemaciclib in hormone receptor positive breast cancer. Oncotarget 2017, 8, 69493-69507, doi:10.18632/oncotarget.17778.

24. Finn, R.S.; Dering, J.; Conklin, D.; Kalous, O.; Cohen, D.J.; Desai, A.J.; Ginther, C.; Atefi, M.; Chen, I.; Fowst, C., et al. PD 0332991, a selective cyclin D kinase 4/6 inhibitor, preferentially inhibits proliferation

of luminal estrogen receptor-positive human breast cancer cell lines in vitro. Breast Cancer Res 2009, 11, R77-R77, doi:10.1186/bcr2419.

25. Teo, Z.L.; Versaci, S.; Dushyanthen, S.; Caramia, F.; Savas, P.; Mintoff, C.P.; Zethoven, M.; Virassamy, B.; Luen, S.J.; McArthur, G.A., et al. Combined CDK4/6 and PI3Kα Inhibition Is Synergistic and Immunogenic in Triple-Negative Breast Cancer. Cancer Res 2017, 77, 6340-6352, doi:10.1158/0008-5472.Can-17-2210.

26. Patnaik, A.; Rosen, L.S.; Tolaney, S.M.; Tolcher, A.W.; Goldman, J.W.; Gandhi, L.; Papadopoulos, K.P.; Beeram, M.; Rasco, D.W.; Hilton, J.F., et al. Efficacy and Safety of Abemaciclib, an Inhibitor of CDK4 and CDK6, for Patients with Breast Cancer, Non-Small Cell Lung Cancer, and Other Solid Tumors. Cancer Discov 2016, 6, 740-753, doi:10.1158/2159-8290.Cd-16-0095.

27. Lilly Reports Topline Results from Phase 3 JUNIPER Trial Evaluating Verzenio™ (abemaciclib) in KRAS-Mutated, Advanced Non-Small Cell Lung Cancer. Availabe online: https://www.prnewswire.com/news-releases/lilly-reports-topline-results-from-phase-3-juniper-trial-evaluating-verzenio-abemaciclib-in-kras-mutated-advanced-non-small-cell-lung-cancer-300533543.html (accessed on 4 Apr 2020).

28. Muzny, D.M.; Bainbridge, M.N.; Chang, K.; Dinh, H.H.; Drummond, J.A.; Fowler, G.; Kovar, C.L.; Lewis, L.R.; Morgan, M.B.; Newsham, I.F., et al. Comprehensive molecular characterization of human

colon and rectal cancer. Nature 2012, 487, 330-337, doi:10.1038/nature11252.

29. O'Leary, B.; Finn, R.S.; Turner, N.C. Treating cancer with selective CDK4/6 inhibitors. Nat Rev Clin Oncol 2016, 13, 417-430, doi:10.1038/nrclinonc.2016.26.

30. Wiedemeyer, W.R.; Dunn, I.F.; Quayle, S.N.; Zhang, J.; Chheda, M.G.; Dunn, G.P.; Zhuang, L.; Rosenbluh, J.; Chen, S.; Xiao, Y., et al. Pattern of retinoblastoma pathway inactivation dictates response to CDK4/6 inhibition in GBM. Proc Natl Acad Sci U S A 2010, 107, 11501-11506, doi:10.1073/pnas.1001613107.

31. Malorni, L.; Piazza, S.; Ciani, Y.; Guarducci, C.; Bonechi, M.; Biagioni, C.; Hart, C.D.; Verardo, R.; Di Leo, A.; Migliaccio, I. A gene expression signature of retinoblastoma loss-of-function is a predictive biomarker of resistance to palbociclib in breast cancer cell lines and is prognostic in patients with ER positive early breast cancer. Oncotarget 2016, 7, 68012-68022, doi:10.18632/oncotarget.12010.

32. Finn, R.S.; Crown, J.P.; Lang, I.; Boer, K.; Bondarenko, I.M.; Kulyk, S.O.; Ettl, J.; Patel, R.; Pinter, T.; Schmidt, M., et al. The cyclin-dependent kinase 4/6 inhibitor palbociclib in combination with letrozole versus letrozole alone as first-line treatment of oestrogen receptor-positive, HER2-negative, advanced breast cancer (PALOMA-1/TRIO-18): a randomised phase 2 study. Lancet Oncol 2015, 16, 25-35, doi:10.1016/s1470-2045(14)71159-3.

33. Finn, R.; Jiang, Y.; Rugo, H.; Moulder, S.L.; Im, S.A.; Gelmon, K.A.; Dieras, V.; Martin, M.; Joy, A.A.; Toi, M., et al. Biomarker analyses from the phase 3 PALOMA-2 trial of palbociclib (P) with letrozole (L) compared with placebo (PLB) plus L in postmenopausal women with ER + /HER2– advanced breast cancer (ABC). Annals of Oncology 2016, 27, vi554, doi:10.1093/annonc/mdw435.05.

34. Donjerkovic, D.; Scott, D.W. Regulation of the G1 phase of the mammalian cell cycle. Cell Research 2000, 10, 1-16, doi:10.1038/sj.cr.7290031.

35. Jansen, V.M.; Bhola, N.E.; Bauer, J.A.; Formisano, L.; Lee, K.M.; Hutchinson, K.E.; Witkiewicz, A.K.; Moore, P.D.; Estrada, M.V.; Sánchez, V., et al. Kinome-Wide RNA Interference Screen Reveals a Role for PDK1 in Acquired Resistance to CDK4/6 Inhibition in ER-Positive Breast Cancer. Cancer Res 2017, 77, 2488-2499, doi:10.1158/0008-5472.Can-16-2653.

36. Herrera-Abreu, M.T.; Palafox, M.; Asghar, U.; Rivas, M.A.; Cutts, R.J.; Garcia-Murillas, I.; Pearson, A.; Guzman, M.; Rodriguez, O.; Grueso, J., et al. Early Adaptation and Acquired Resistance to CDK4/6 Inhibition in Estrogen Receptor-Positive Breast Cancer. Cancer Res 2016, 76, 2301-2313, doi:10.1158/0008-5472.Can-15-0728.

37. O'Brien, T.; Xiao, Y.; Ong, C.; Daemen, A.; Friedman, L. Abstract P3-04-24: Identification of preclinical mechanisms driving acquired resistance to selective ERa degraders (SERDs), CDK4/6 inhibitors, or to combinations of both agents. Cancer Research 2017, 77, P3-04-24-P03-04-24, doi:10.1158/1538-7445.Sabcs16-p3-04-24.

38. Ligresti, G.; Militello, L.; Steelman, L.S.; Cavallaro, A.; Basile, F.; Nicoletti, F.; Stivala, F.; McCubrey, J.A.; Libra, M. PIK3CA mutations in human solid tumors: role in sensitivity to various therapeutic approaches. Cell Cycle 2009, 8, 1352-1358, doi:10.4161/cc.8.9.8255.

39. Janku, F.; Yap, T.A.; Meric-Bernstam, F. Targeting the PI3K pathway in cancer: are we making headway? Nat Rev Clin Oncol 2018, 15, 273-291, doi:10.1038/nrclinonc.2018.28.

40. Ihle, N.T.; Lemos, R., Jr.; Wipf, P.; Yacoub, A.; Mitchell, C.; Siwak, D.; Mills, G.B.; Dent, P.; Kirkpatrick, D.L.; Powis, G. Mutations in the phosphatidylinositol-3-kinase pathway predict for antitumor activity of the inhibitor PX-866 whereas oncogenic Ras is a dominant predictor for resistance. Cancer Res 2009, 69, 143-150, doi:10.1158/0008-5472.Can-07-6656.

41. Furet, P.; Guagnano, V.; Fairhurst, R.A.; Imbach-Weese, P.; Bruce, I.; Knapp, M.; Fritsch, C.; Blasco, F.; Blanz, J.; Aichholz, R., et al. Discovery of NVP-BYL719 a potent and selective phosphatidylinositol-3 kinase alpha inhibitor selected for clinical evaluation. Bioorg Med Chem Lett 2013, 23, 3741-3748, doi:10.1016/j.bmcl.2013.05.007.

42. Iida, M.; Nakamura, M.; Tokuda, E.; Niwa, T.; Ishida, T.; Hayashi, S.-I. Abstract P6-04-02: CDK6 might be a key factor for efficacy of CDK4/6 inhibitor and the hormone sensitivity following acquired resistance. Cancer Research 2018, 78, P6-04-02-P06-04-02, doi:10.1158/1538-7445.Sabcs17-p6-04-02.

43. O'Brien, N.; Conklin, D.; Beckmann, R.; Luo, T.; Chau, K.; Thomas, J.; Mc Nulty, A.; Marchal, C.; Kalous, O.; von Euw, E., et al. Preclinical Activity of Abemaciclib Alone or in Combination with Antimitotic and Targeted Therapies in Breast Cancer. Mol Cancer Ther 2018, 17, 897-907, doi:10.1158/1535-7163.Mct-17-0290.

44. Zhang, J.; Xu, K.; Liu, P.; Geng, Y.; Wang, B.; Gan, W.; Guo, J.; Wu, F.; Chin, Y.R.; Berrios, C., et al. Inhibition of Rb Phosphorylation Leads to mTORC2-Mediated Activation of Akt. Mol Cell 2016, 62, 929-942, doi:10.1016/j.molcel.2016.04.023.

45. Knudsen, E.S.; Witkiewicz, A.K. The Strange Case of CDK4/6 Inhibitors: Mechanisms, Resistance, and Combination Strategies. Trends Cancer 2017, 3, 39-55, doi:10.1016/j.trecan.2016.11.006.

46. Forero-Torres, A.; Han, H.; Dees, E.C.; Wesolowski, R.; Bardia, A.; Kabos, P.; Layman, R.M.; Lu, J.M.; Kern, K.A.; Perea, R., et al. Phase Ib study of gedatolisib in combination with palbociclib and endocrine therapy (ET) in women with estrogen receptor (ER) positive (+) metastatic breast cancer (MBC) (B2151009). Journal of Clinical Oncology 2018, 36, 1040-1040, doi:10.1200/JCO.2018.36.15_suppl.1040.

47. Pascual, J.; MacPherson, I.R.; Armstrong, A.C.; Ward, S.E.; Parmar, M.; Turner, A.J.; Bye, H.; Proszek, P.; Dodson, A.; Garcia-Murillas, I., et al. PIPA: A phase Ib study of β-isoform sparing phosphatidylinositol 3-kinase (PI3K) inhibitor taselisib (T) plus palbociclib (P) and fulvestrant (FUL) in PIK3CA-mutant (mt) ER-positive and taselisib (T) plus palbociclib (P) in PIK3CA-mutant (mt) ER-negative advanced breast cancer. Journal of

Clinical Oncology 2019, 37, 1051-1051, doi:10.1200/JCO.2019.37.15_suppl.1051.

48. Munster, P.N.; Hamilton, E.P.; Franklin, C.; Bhansali, S.; Wan, K.; Hewes, B.; Juric, D. Phase lb study of LEE011 and BYL719 in combination with letrozole in estrogen receptor-positive, HER2-negative breast cancer (ER+, HER2− BC). Journal of Clinical Oncology 2014, 32, 533-533, doi:10.1200/jco.2014.32.15_suppl.533.

49. Mizrachi, A.; Dunn, L.; Ho, A.; Scaltriti, M. Abstract 61: Overcoming acquired resistance to PI3K inhibitors in head and neck squamous cell carcinoma with combination treatment. Clinical Cancer Research 2017, 23, 61-61, doi:10.1158/1557-3265.Aacrahns17-61.

국문초록

인간 대장암 세포주에 대한 선택적 CDK4/6 억제제의 항종양효과와 작용기전에 대한 연구

목적: 대장암은 전 세계적으로 세 번째로 흔한 악성종양이며, 대장암으로 인한 사망률은 암사망률 중 두 번째로 높은 것으로 알려져 있다. 이미 다양한 악성 종양에서 암세포의 세포주기를 조절하는 선택적 CDK4/6 억제제가 새로운 치료적 대안으로 떠오르고 있음에도 불구하고, 아직까지 대장암의 치료에 있어 세포주기를 조절하는 약제에 대한 연구는 부족한 실정이다. 본 연구는 대장암 세포주에서 선택적 CDK4/6 억제제의 항종양효과를 확인하고, 약물의 작용기전을 탐구하기 위해 설계 되었다.

재료 및 방법: 대장암 세포주에 대하여 세 가지 선택적 CDK4/6 억제제들 (palbociclib, abemaciclib, ribociclib)의 항종양효과를 확인하였다. 그 중 가장 효과적인 선택적 CDK4/6 억제제를 가지고 대장암 세포주에 대한 약물의 작용 기전을 탐구하고

최적의 병합요법제제를 찾아내기 위한 실험을 진행하였다. 최종적으로 무흉선 누드 마우스를 사용한 종양이종이식모델을 통해 체내에서의 병합 요법의 효과를 확인하였다.

결과: 다양한 대장암 세포주에 대한 종양 성장 억제 실험을 통해 선택적 CDK4/6 억제제인 palbociclib, abemaciclib, ribociclib 중 abemaciclib 이 다른 선택적 CDK4/6 억제제에 비해 가장 강력한 항종양효과를 가지는 것으로 확인되었다. *KRAS* 의 돌연변이가 없는 대장암 세포주들이 *KRAS* 돌연변이를 가진 세포주에 비해 abemaciclib 에 감수성을 보이는 경향도 확인하였다. 실험에 사용된 대장암 세포주 중 Abemaciclib 에 가장 감수성이 높은 Caco-2 와 SNU-C4 대장암 세포주에서 확인한 결과 abemaciclib 은 단독 사용 시 세포 주기의 진행 및 세포의 증식을 억제하였다. 또한, abemaciclib 단독 치료에 대한 치료 저항성 발생과정에 CDK2-cyclin E 복합체에 의한 Rb 인산화와 AKT 인산화가 관여하고 있음을 확인하였다. Abemaciclib 과 BYL719 (선택적 PI3K p110α 억제제)의 병합요법은 abemaciclib 단독 치료의 저항 발생 기전을 극복할 수 있는 가능한 병합요법임을 체외 및 체내 실험 모델을 통해 확인하였다. Abemaciclib 과 BYL719 의 병합효과는 *PIK3CA* 돌연변이가 있는 대장암 세포주에서 더 두드러지게 나타났다. 이 병합요법은 세포성장 억제, 세포주기정지, 세포이동억제 등의 기전을 통해 항종양효과를 나타내는 것으로 체외 실험을 통해 밝혀졌다. *PIK3CA* 돌연변이가 있는 SNU-C4 대장암 세포주를 가지고 만든 종양이종이식 모델에서는 abemaciclib 과 BYL719 의

병합요법이 적절한 독성 범위 내에서 종양의 성장 억제뿐만 아니라 암세포의 세포자멸사를 유도하는 것을 관찰할 수 있었다.

결론: Abemaciclib 단독 요법은 인간 대장암 세포주에서 항종양효과를 가지는 것으로 확인되었다. 또한, 선택적 PI3K p110α 와 CDK4/6 의 이중 억제는 인간 대장암 세포주에서 항종양 효과를 상승시키는 것으로 나타났다. *PIK3CA* 돌연변이는 이 병합요법에 대한 반응을 예측할 수 있는 추가적인 생물학적 표지자로서의 가능성을 보여 주었다. 선택적 PI3K p110α 와 CDK4/6 의 이중 억제는 진행성 대장암을 가진 환자들에게 필요한 새로운 치료적 대안을 제시할 수 있을 것으로 보인다.

주요어: 대장암, 아베마시클립 (Abemaciclib), BYL719 (Alpelisib), 세포주기, 세포이동, 세포자멸사, *PIK3CA*

학 번 : 2013 - 30599